PHILOSOPHICAL TRANSACTIONS OF THE ROYAL SOCIETY A MATHEMATICAL, PHYSICAL & ENGINEERING SCIENCES

Osmotically driven intracellular transport phenomena

Richard P. Batycky, Roy Hammerstedt and David A. Edwards

Phil. Trans. R. Soc. Lond. A 1997 **355**, 2459-2487
doi: 10.1098/rsta.1997.0143

Osmotically driven intracellular transport phenomena

By Richard P. Batycky[1]†, Roy Hammerstedt[2] and David A. Edwards[1]

[1]*Department of Chemical Engineering,* [2]*Department of Biochemistry, Penn State University, University Park, PA 16802, USA*

Contents

		PAGE
1.	Introduction	2460
	(*a*) Definition of concentration variables	2461
2.	Cellular velocity distribution	2463
3.	Cellular transport theorem	2464
4.	Cell membrane motion: water transport	2466
5.	Transmembrane solute transport	2466
6.	Salt response	2467
	(*a*) Cellular concentration distribution	2468
	(*b*) Volume evolution	2469
	(*c*) Hydraulic permeability L_{p}	2470
	(*d*) Boyle van't Hoff relationship	2471
7.	Salt and semipermeable solute response	2472
	(*a*) Cellular concentration distribution	2473
	(*b*) Volume evolution	2475
	(*c*) Effective semipermeable solute diffusivity	2476
	(*d*) Predicting kinetic volume changes: hepatocyte base case	2477
	(*e*) Experimental protocol for the determination of k, P_{sp} and L_{p}	2480
	(*f*) Comparison with former model: human sperm	2483
8.	Arbitrary cell shapes and future directions	2484
	References	2487

A theory of cell-volume response to abrupt or gradual changes in extracellular osmotic conditions is outlined. The coupled transport of water and impermeable and semipermeable solutes is considered. Semipermeable solutes, including relatively small lipophilic molecules, like glycerol or urea, are permitted to absorb to the membranes of internal organelle bodies, where they diffuse with a configuration-specific lateral diffusion coefficient. Impermeable solutes (such as salts) are excluded from internal organelles, resulting in a significant osmotically inactive cell-volume fraction. Cell-volume expansion or contraction in response to anisosmotic conditions is shown to depend strongly on the internal absorption behaviour of semipermeable solutes, as well as upon membrane permeation parameters. The results of the analysis

† Present address: 528 Chemical-Mineral Engineering Building, University of Alberta, Canada T6G 2G6.

Phil. Trans. R. Soc. Lond. A (1997) **355**, 2459–2488
Printed in Great Britain

lay the foundations for accurate determination of membrane permeability variables, of importance to a variety of cellular transport processes, including those involved in cell cryopreservation.

1. Introduction

Present understanding of cellular response to osmotic stimuli derives largely from observations of cell volume changes (Liu *et al.* 1995) and lysis (Gao *et al.* 1992) following exposure of cells to osmotic stresses. These responses have, at least in part, been successfully attributed to the relative permeability of cell membranes to water and membrane-penetrating solutes, such as glycerol and ethylene glycol (Gilmore *et al.* 1995). However, many osmotic phenomena of major importance to the health of the cell have yet to be fully understood—or quantified in a way that makes existing understanding predictive; these phenomena include the effects of osmotic stresses on the cellular and transmembrane transport of membrane-permeable or semipermeable molecules, the role of permeant absorption to internal organelle membranes, the reversibility of biochemical changes caused by osmotic stresses and the effects of osmotic stresses on metabolic intracellular reactions. This article aims to address some of these outstanding questions.

The basic problem that is addressed concerns the radial dilatation of a spherical cell membrane that accompanies a sudden or gradual change in extracellular salt or semipermeable solute concentration. Owing to the fluidity of animal cell membranes (as well as bacteria and many protozoa), combined with their innate impermeability to small ions, hypertonic (high salt) and hypotonic (low salt) conditions in the extracellular environment can produce substantial osmotic stresses whose effects are to cause the plasma membrane to shrink or expand. While most cell membranes possess special transport mechanisms to relieve osmotic imbalances (e.g. sodium and potassium ATPases), very large osmotic imbalances are possible in physiological conditions that cannot be relieved sufficiently rapidly by membrane transport processes prior to cell shape change. For example, inhaled liquid aerosols often enter the mouth at isosmotic conditions, however, owing to the high humidity in the airways, they can become increasingly hypotonic as they penetrate deeper into the airways and alveoli. Deposition on lung epithelia of these hypotonic solutions can result in expansion of epithelial cells, potentially lysing epithelial cells or permeabilizing the epithelial barrier (Patton 1996).

An obvious application of this work is towards the development of protocols for the cryopreservation of living cells. The cryopreservation of human, animal and plant cells depends critically upon the ability of cells to survive osmotic stresses, such as arise during freezing and thawing protocols (Hammerstedt *et al.* 1990). The cryopreservation of human blood, elite or endangered germ plasma and plant cells or organs (often derived by genetically modified plant tissue cultures)—each provide important examples where cells are exposed to significant osmotic stresses. Major questions that remain unanswered as regards the success of freezing and thawing protocols in the cryopreservation industry relate to the irreversibility of membrane structural changes after thawing (Carruthers & Melchior 1988; Quinn 1989; Foote 1984), the localization of cryoprotectant in internal and external cell membranes (O'Leary & Levin 1984; Bashford *et al.* 1986; Hammerstedt *et al.* 1990), intracellular

structural changes following cryopreservation (Courtens & Paquignon 1985) and the reason(s) for the need to impose dissimilar thawing and freezing kinetics (Mazur *et al.* 1984; Watson 1990). Each of these questions requires a more complete understanding of water and solute transport into and out of cells in anisosmotic conditions. Lacking this understanding, freezing and thawing of cells is performed by 'matching' the rates of freezing and thawing kinetics (Mazur 1984), without a clear knowledge of why, with the result that progress toward optimization of cryopreservation protocols has been limited.

Our attention in this study is strictly to the theoretical description of spherical cells undergoing radial expansions and contractions owing to homogeneous osmotic imbalances. Cells, however, can be of a variety of shapes, including cylindrical and disk-like shapes, osmotic stresses may be inhomogeneous, and molecules such as salts, that are *impermeable* on a short time scale, may be *permeable* on a longer time scale owing to ion transporters and other active transport processes. Our aim in restricting our focus in this article is to provide a sufficiently detailed consideration so that generalization to other scenarios can be relatively straightforwardly made in the future. In terms of practical utility, a companion article (Batycky *et al.* 1998) provides a paradigmatic application of this work for interpretation of osmotic challenge experiments, particularly as an aid in the development of cryopreservation protocols.

The arrangement of this article is as follows: having defined basic concentration variables in the remainder of § 1, cell velocity variables are defined (§ 2), and in § 3 the kinematics of non-material membrane motion are quantified. In §§ 4 and 5, water, salt and semipermeable solute transport is considered. The main development of cell volume response to salt and semipermeable solute changes is considered in §§ 6 and 7, respectively. A discussion of results and generalization to more diverse conditions is provided in §§ 7 and 8.

(*a*) *Definition of concentration variables*

Consider a cell of volume V containing N_{salt} moles of salt distributed uniformly throughout the cell interior, or cytosol. We define the mean salt concentration $\overline{C}^{\mathrm{i}}_{\mathrm{salt}}$ as

$$\overline{C}^{\mathrm{i}}_{\mathrm{salt}} = \frac{\text{moles of salt}}{\text{total cell volume}} = \frac{N_{\mathrm{salt}}}{V}, \tag{1.1}$$

meaning that the cell is regarded as a homogeneous body throughout which salt can be distributed. However, owing to the inability of salt (or possibly semipermeable solute) to penetrate various organelles of the cell, a finite 'non-osmotically' active volume V_{b} exists within the cell, so that the actual concentration within the cytosol, in the conditions considered here, is

$$C^{\mathrm{i}}_{\mathrm{salt}} = \frac{\text{moles of salt}}{\text{cytosol or osmotically active volume}} = \frac{N_{\mathrm{salt}}}{V - V_{\mathrm{b}}}. \tag{1.2}$$

It is apparent that these two concentrations are related by

$$\overline{C}^{\mathrm{i}}_{\mathrm{salt}} = C^{\mathrm{i}}_{\mathrm{salt}}(1 - \phi), \tag{1.3}$$

where $\phi = V_{\mathrm{b}}/V$ is the volume fraction of osmotically inactive intracellular compartments (or organelles).

Consider now a second semipermeable solute (sp), that absorbs very rapidly to internal organelle membranes (of total membrane area s_{m}) of the cell. In equilibrium

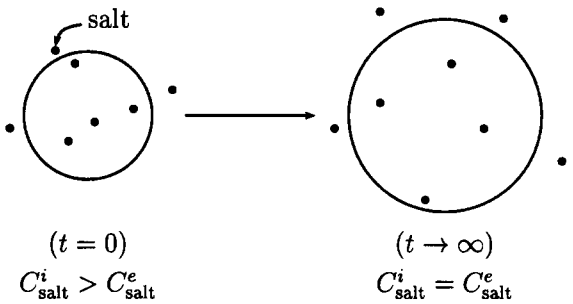

Figure 1. A qualitative response of a cell subjected to hyposmotic conditions. At time $t = 0$, the cell has a higher internal salt concentration $C^{\mathrm{i}}_{\mathrm{salt}}$ than that of the surounding medium $C^{\mathrm{e}}_{\mathrm{salt}}$. As a result, the cell expands until the two concentrations are equalized.

conditions, the mean semipermeable solute cell concentration is

$$\overline{C}^{\mathrm{i}}_{\mathrm{sp}} = N_{\mathrm{sp}}/V, \tag{1.4}$$

whereas the semipermeable solute concentration $C^{\mathrm{i}}_{\mathrm{sp}}$ uniformly distributed throughout the cytosol, and absorbed to internal membranes with Henry's law absorption coefficient k, is given by

$$C^{\mathrm{i}}_{\mathrm{sp}}(V - V_{\mathrm{b}}) + C^{\mathrm{i}}_{\mathrm{sp}} k s_{\mathrm{m}} + C^{\mathrm{i}}_{\mathrm{sp}} K V_{\mathrm{b}} = N_{\mathrm{sp}}, \tag{1.5}$$

whence

$$\overline{C}^{\mathrm{i}}_{\mathrm{sp}} = C^{\mathrm{i}}_{\mathrm{sp}}(1 - \phi + k\alpha + K\phi), \tag{1.6}$$

with $\alpha = s_{\mathrm{m}}/V$ the specific surface area of organelle membranes and K the partition coefficient into the organelles. While equations (1.3) and (1.6) have been defined here in equilibrium, point-wise counterparts can be derived in non-equilibrium conditions of identical form (Edwards & Davis 1995), hence equations (1.3) and (1.6) will be used subsequently in both equilibrium and non-equilibrium conditions. Particularly, $\overline{C}^{\mathrm{i}}_{\mathrm{sp}}$ and $\overline{C}^{\mathrm{i}}_{\mathrm{salt}}$ will be regarded as volume integrals over a cellular volume that is small compared to the cell size though large compared to the volume of an organelle. Given that a characteristic organelle dimension is 100 nm (see § 7 *d*) and that of the cell $\approx 10\,\mu\mathrm{m}$, this implies a cellular volume average over a volume *ca.* $0.26\,\mu\mathrm{m}^3$, which is much larger than the organelle volume (*ca.* $4 \times 10^{-3}\,\mu\mathrm{m}^3$) and smaller than the cell volume (*ca.* $4189\,\mu\mathrm{m}^3$).

Consider, for simplicity, the transient evolution of a spherical cell from one volume to another in hyposmotic conditions, as in figure 1. Initially, the salt concentration inside the cell $C^{\mathrm{i}}_{\mathrm{salt}}$ is larger than in the extracellular fluid $C^{\mathrm{e}}_{\mathrm{salt}}$. This gives rise to a higher osmotic pressure inside the cell, which in turn causes the cell to expand as water enters the cell, ultimately diluting the internal salt concentration until the two are equal. While the initial and final volumes are given by (1.2), the dependence of the transient volume evolution upon the hydraulic membrane permeability L_{p}, among other transport properties, remains to be determined.

In the presence of a semipermeable solute, such as a cryoprotectant, this transient evolution is rather more complex. Consider, as an example, the final stage of a typical thawing cycle (figure 2) when cryoprotectant is removed from a thawed cell. Initially, the salt concentrations both inside and outside the cell are equal, however, there is cryoprotectant within the cell while there is none in the isosmotic bath. This configuration causes the cell to initially expand as a result of the higher (semipermeable)

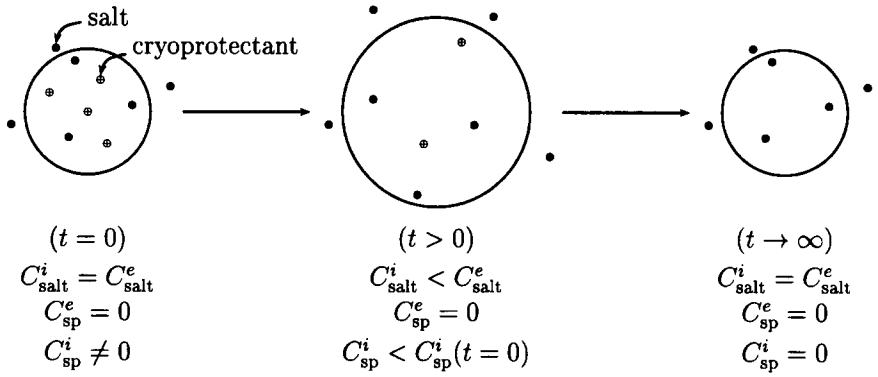

Figure 2. The qualitative response of a cell in the presence of a cryoprotectant. This is an example of a thawing cycle, where at time $t = 0$ the cell containing cryoprotectant is immersed in a fully thawed isosmotic bath. Initially the cell expands due to its higher concentration of intracellular cryoprotectant. This expansion is reversed both due to the lower concentration of salt within the cell and the transport of cryoprotectant out of the cell. Ultimately, the cell reverts back to its original size as all the cryoprotectant has escaped.

cryoprotectant concentration within the cell $C^{\mathrm{i}}_{\mathrm{sp}}$ relative to the bath $C^{\mathrm{e}}_{\mathrm{sp}} \cong 0$. This expansion is ultimately reversed both due to the now lower salt concentration within the cell and the escape of cryoprotectant across the cell membrane and into the bath. Eventually, the cell attains its original size when all the cryoprotectant has escaped. This transient behaviour will depend not only on the hydraulic permeability L_{p}, but on cryoprotectant membrane properties such as the reflection coefficient σ and the permeability P_{sp}. A dependence upon the intracellular cryoprotectant diffusivity $\overline{D}^*_{\mathrm{sp}}$ will also be observed.

In the next sections, appropriate governing equations and boundary conditions are developed to describe this dynamic cellular problem, following which analytical and numerical solutions are obtained describing the cell volume response to anisosmotic conditions of the kind discussed here.

2. Cellular velocity distribution

A major question that must first be answered concerns whether the response of a spherical cell to anisosmotic conditions is convectively or diffusively driven. Figure 3 shows a spherical coordinate system geometrically centred within a cell. The cell is assumed to be a perfect sphere with radius R. Because of the symmetry of the cell and the fact that a uniform expansion or contraction of the cell in the r-direction preserves this symmetry, the resultant velocity field is independent of θ and ϕ. This uniform expansion implicitly requires that the membrane properties L_{p}, σ and P_{sp} are also independent of position along the membrane. Furthermore, the expansion or contraction strictly in the r-direction does not give rise to flow in the θ- or ϕ-directions, i.e. $v_\theta = v_\phi = 0$. The fluid velocity profile within the cell may then be generally represented by

$$\boldsymbol{v} = \boldsymbol{i}_r v_r(r). \tag{2.1}$$

Since the cytosolic fluid is incompressible, the continuity equation along with (2.1) gives

$$\nabla \cdot \boldsymbol{v} = \frac{1}{r^2}\frac{\mathrm{d}}{\mathrm{d}r}(r^2 v_r) = 0, \tag{2.2}$$

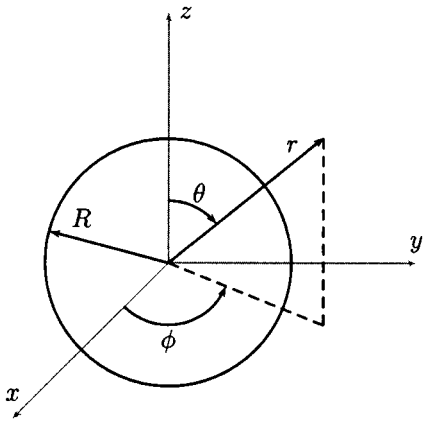

Figure 3. Spherical coordinate system placed at the centre of an idealized cell. The cell has a radius R.

which has the solution

$$v_r(r) = A/r^2, \tag{2.3}$$

with A an arbitrary constant. To avoid the singularity at $r = 0$, we require $A = 0$. This yields the somewhat trivial but important result

$$\boldsymbol{v} = \boldsymbol{0}, \tag{2.4}$$

at least for this simplified cell geometry. This means that the fluid *does not move* as a consequence of an osmotic expansion or contraction of the cell membrane, rather the membrane simply sweeps out the intra- or extra-cellular fluid as a consequence of osmotic stresses exerted on the membrane. Of course, to an observer situated on the moving membrane, the water nonetheless *appears* to be in motion. Thus, the single driving force for redistribution of solutes in this problem is molecular diffusion.

Note that upon expansion or contraction of the cell membrane, the movement of organelles within the cytosol is driven entirely by diffusion. That is, there exists no tethering of organelles to the plasma membrane. The problem therefore differs in this respect from the related problem of an expanding porous body considered by Frankel *et al.* (1991). In their problem, expansion of the porous 'solid' gives rise to redistribution of the interstitial fluid by *convection*. It is furthermore noteworthy that the organelles are neutrally buoyant, whence convection induced by diffusion as treated by Camacho & Brenner (1995) is not a source of concern. Solute diffusion may introduce a second-order velocity effect. However, as attention will subsequently be constrained to low Peclet circumstances, this second-order contribution lies beyond the scope of our analysis.

3. Cellular transport theorem

The various boundary conditions required at the moving cell boundary can be derived in the form of a generalized Reynolds transport law (Aris 1960). Figure 4 shows the cell and associated control volume over which mass and mole balances are ultimately to be formed. Although the problem considered here is purely diffusive ($\boldsymbol{v} = \boldsymbol{0}$), the membrane velocity $\boldsymbol{u}$ is non-zero; in other words, the membrane is *non-material*.

Let $\psi(\boldsymbol{r}, t)$ represent a continuous volumetric density field (such as mass density,

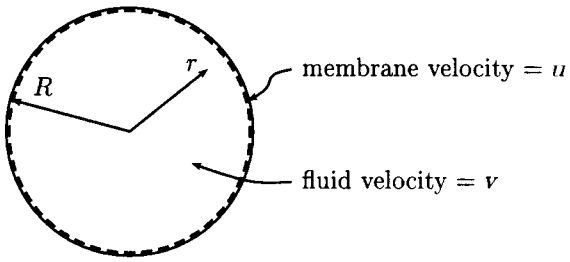

Figure 4. The non-material control volume across which mass is exchanged. This non-material nature is characterized by a membrane velocity $\boldsymbol{u}$ which is different than the mass average or fluid velocity $\boldsymbol{v}$ at the cell surface $r = R$. The control volume has a volume $\mathcal{V}(t)$ bound by the surface $\partial\mathcal{V}(t)$.

ρ, or semipermeable solute concentration $\overline{C}^{\mathrm{i}}_{\mathrm{sp}}$). The total amount of the property $\Psi(t)$ within the control volume $\mathcal{V}(t)$ is given by

$$\Psi(t) \stackrel{\mathrm{def}}{=} \int_{\mathcal{V}(t)} \psi(\boldsymbol{r}, t)\, \mathrm{d}V. \tag{3.1}$$

For a non-material interface the Reynolds transport theorem can be stated as

$$\frac{\mathrm{d}\Psi}{\mathrm{d}t} = \int_{\mathcal{V}(t)} \left(\frac{\partial \psi}{\partial t} + \boldsymbol{v} \cdot \nabla \psi \right) \mathrm{d}V + \int_{\partial\mathcal{V}(t)} \mathrm{d}\boldsymbol{S} \cdot (\boldsymbol{u} - \boldsymbol{v}) \psi, \tag{3.2}$$

which is a sum of contributions arising from the time-rate of change of ψ within the volume $\mathcal{V}$, convection of ψ across the membrane at the mass average velocity $\boldsymbol{v}$ ($= \boldsymbol{0}$ in the present case), and transport of ψ across the membrane due to a difference in the mass average and membrane velocities.

Assuming the relevant symmetry conditions discussed previously (along with $\boldsymbol{v} = \boldsymbol{0}$ and $\boldsymbol{u} = \boldsymbol{i}_r u(t)$), equations (3.1) and (3.2) assume the simpler forms

$$\Psi(t) = 4\pi \int_0^{R(t)} \psi(r, t) r^2\, \mathrm{d}r \tag{3.3}$$

and

$$\frac{\mathrm{d}\Psi(t)}{\mathrm{d}t} = 4\pi \int_0^{R(t)} \frac{\partial \psi(r, t)}{\partial t} r^2\, \mathrm{d}r + 4\pi R(t)^2 u(t) \psi(R(t), t). \tag{3.4}$$

We first imagine the volumetric property $\psi(r, t)$ to be the mass density ρ of the fluid. Setting $\psi = \rho = \text{const.}$ in (3.3) and (3.4) produces

$$\frac{\mathrm{d}R}{\mathrm{d}t} = u, \tag{3.5}$$

which is correct by definition. This result assumes the presence of salt and semipermeable solute does not change the mass density of the cytosolic fluid appreciably.

Next we take $\psi(r, t) = \overline{C}(r, t)$, where the field $\overline{C}$ may be taken to represent either $\overline{C}^{\mathrm{i}}_{\mathrm{salt}}$ or $\overline{C}^{\mathrm{i}}_{\mathrm{sp}}$. The field $\overline{C}$ satisfies a diffusion equation within the cell (Brenner & Edwards 1993), namely

$$\frac{\partial \overline{C}}{\partial t} = \frac{1}{r^2} \frac{\partial}{\partial r} \left(\overline{D}^* r^2 \frac{\partial \overline{C}}{\partial r} \right). \tag{3.6}$$

In evaluating (3.4) with this choice of ψ, $\Psi(t) = N(t)$ is the total number of moles

of salt or semipermeable solute within the cell. Substitution into (3.3) and (3.4) along with use of the divergence theorem yields

$$\frac{\mathrm{d}N}{\mathrm{d}t} = 4\pi R^2 \left(\overline{D}^* \frac{\partial \overline{C}}{\partial r} + uC \right) \Big|_{r=R}. \tag{3.7}$$

The quantity appearing in parentheses above is the flux (per unit area) of either salt or cryoprotectant at the membrane *into* the cell. In the case of salt, this flux is *zero*, whereas in the case of semipermeable solute this flux must be related to a kinematical relationship involving the relevant membrane properties, as next discussed. The equivalence $\overline{C} = C$ (or $\phi = 0$) at $r = R$ has been made in (3.7), reflecting the absence of organelles near the cell plasma membrane on account of the cell cortex.

4. Cell membrane motion: water transport

The driving force for membrane motion is a difference in net osmotic pressure on either side of the membrane. This pressure is defined as

$$\Pi = CR_{\mathrm{gas}}T, \tag{4.1}$$

with C the salt or semipermeable solute concentration (or the sum of both), R_{gas} the gas constant ($R_{\mathrm{gas}} = 82.06$ cm^3 atm mol^{-1} K^{-1}) and T the absolute temperature. For an observer fixed on the membrane, the water passes through the membrane with velocity $-u$. This velocity can be related to the osmotic pressure difference via a Darcy's law type relationship (Darcy 1856) characterized by a hydraulic permeability L_{p}. In the absence of cryoprotectant, the relationship (noting (3.5) and the discussion preceeding (3.7)) is given by

$$\frac{\mathrm{d}R}{\mathrm{d}t} = -L_{\mathrm{p}}R_{\mathrm{gas}}T(C^{\mathrm{e}}_{\mathrm{salt}} - C^{\mathrm{i}}_{\mathrm{salt}}|_{r=R(t)}). \tag{4.2}$$

With a semipermeable solute present, an additional contribution to the osmotic pressure arises. Since the semipermeable solute is presumed capable of crossing the membrane, though not without steric hindrance, a filtration coefficient σ is included to account for the ease at which the semipermeable solute can pass through the membrane. The value $\sigma = 1$ denotes a solute that is completely rejected by the membrane (as is the case with salt), while $\sigma = 0$ implies resistance-free passage of the solute across the membrane. The velocity u with which the membrane moves is then

$$\frac{\mathrm{d}R}{\mathrm{d}t} = -L_{\mathrm{p}}R_{\mathrm{gas}}T[(C^{\mathrm{e}}_{\mathrm{salt}} - C^{\mathrm{i}}_{\mathrm{salt}}|_{r=R(t)}) + \sigma(C^{\mathrm{e}}_{\mathrm{sp}} - C^{\mathrm{i}}_{\mathrm{sp}}|_{r=R(t)})]. \tag{4.3}$$

5. Transmembrane solute transport

The flux of salt across the membrane is assumed always to be zero. From (3.7) this gives the boundary condition imposed upon $C^{\mathrm{i}}_{\mathrm{salt}}$ at the membrane surface, namely

$$\overline{D}^*_{\mathrm{salt}} \frac{\partial \overline{C}^{\mathrm{i}}_{\mathrm{salt}}}{\partial r} + uC^{\mathrm{i}}_{\mathrm{salt}} = 0, \quad \forall (r = R(t), t). \tag{5.1}$$

In the presence of semipermeable solute, however, a kinematical relationship for the flux across the membrane must be derived. For this purpose, following an analysis like that of Diamond & Katz (1974), consider an observer sitting on the membrane

(figure 5). The membrane has thickness ℓ, diffusivity D^{m} and filtration coefficient σ. Assuming the membrane thickness ℓ to be much smaller than the membrane curvature radius R, the steady-state convection–diffusion equation across the membrane can be written as

$$u'(1-\sigma)\frac{\mathrm{d}C}{\mathrm{d}x'} = D^{\mathrm{m}}\frac{\mathrm{d}^2C}{\mathrm{d}x'^2}, \tag{5.2}$$

along with the boundary conditions $C = C^{\mathrm{i}}_{\mathrm{sp}}$ at $x' = 0$ and $C = C^{\mathrm{e}}_{\mathrm{sp}}$ at $x' = \ell$. The solution for the flux (which is constant at all x' positions in pseudosteady-state) is determined to be

$$u'(1-\sigma)C - D^{\mathrm{m}}\frac{\mathrm{d}C}{\mathrm{d}x} = -u'(1-\sigma)\left(\frac{C^{\mathrm{i}}_{\mathrm{sp}} - C^{\mathrm{e}}_{\mathrm{sp}}}{1-\mathrm{e}^{u'(1-\sigma)\ell/D^m}} - C^{\mathrm{i}}_{\mathrm{sp}}\right). \tag{5.3}$$

With respect to a reference frame fixed in the cell as opposed to the membrane, the velocity is simply

$$u' = -u. \tag{5.4}$$

This fact along with the requirement of continuity of flux at the cell membrane boundary enables (3.7) to be written as

$$\overline{D}^*_{\mathrm{sp}}\frac{\partial\overline{C}^{\mathrm{i}}_{\mathrm{sp}}}{\partial r} + uC^{\mathrm{i}}_{\mathrm{sp}} = u(1-\sigma)\left(\frac{C^{\mathrm{e}}_{\mathrm{sp}} - C^{\mathrm{i}}_{\mathrm{sp}}}{1-\mathrm{e}^{-u(1-\sigma)\ell/D^m}} + C^{\mathrm{i}}_{\mathrm{sp}}\right), \quad \forall(r = R(t), t). \tag{5.5}$$

This can be expressed in a more familiar form by first defining

$$P_{\mathrm{sp}} \stackrel{\mathrm{def}}{=} D^{\mathrm{m}}/\ell, \tag{5.6}$$

as the semipermeable solute permeability and examining the case where u is small relative to P_{sp}. Let Pe_{m} be the membrane Peclet number representing the ratio of convective to diffusive driving forces and defined as

$$Pe_{\mathrm{m}} \stackrel{\mathrm{def}}{=} \frac{u(1-\sigma)}{P_{\mathrm{sp}}} \ll 1. \tag{5.7}$$

The flux condition may be rewritten as

$$\overline{D}^*_{\mathrm{sp}}\frac{\partial\overline{C}^{\mathrm{i}}_{\mathrm{sp}}}{\partial r} + uC^{\mathrm{i}}_{\mathrm{sp}} = P_{\mathrm{sp}}[C^{\mathrm{e}}_{\mathrm{sp}} - C^{\mathrm{i}}_{\mathrm{sp}} + Pe_{\mathrm{m}}(\tfrac{1}{2}C^{\mathrm{e}}_{\mathrm{sp}} + C^{\mathrm{i}}_{\mathrm{sp}}) + \mathcal{O}(Pe^2_{\mathrm{m}})]. \tag{5.8}$$

Thus, limiting our analysis to small membrane Peclet number (of relevance to the problem at hand) gives the relationship

$$\overline{D}^*_{\mathrm{sp}}\frac{\partial\overline{C}^{\mathrm{i}}_{\mathrm{sp}}}{\partial r} + uC^{\mathrm{i}}_{\mathrm{sp}} = P_{\mathrm{sp}}(C^{\mathrm{e}}_{\mathrm{sp}} - C^{\mathrm{i}}_{\mathrm{sp}}), \quad \forall(r = R(t), t), \tag{5.9}$$

which is the usual form of the kinematical membrane transport condition (Gilmore *et al.* 1995).

6. Salt response

In this and following subsections, the volumetric response of an isolated spherical cell due to a sudden spatially uniform change in the external bath salt concentration will be considered, employing equations derived previously. The governing differential

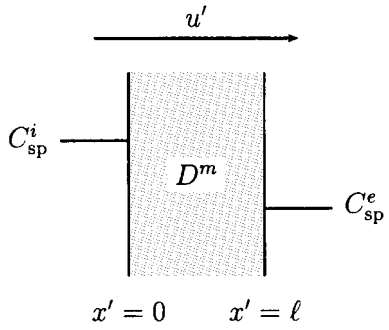

Figure 5. An idealized view of the cell membrane relative to an observer fixed on the membrane. The water appears to flow from lower to higher concentrations. The membrane is characterized by a diffusivity D^{m}, thickness ℓ and filtration coefficient σ.

equation inside the cell is (cf. (3.6))

$$\frac{\partial \overline{C}^{\mathrm{i}}_{\mathrm{salt}}}{\partial t} = \frac{1}{r^2}\frac{\partial}{\partial r}\left(\overline{D}^{*}_{\mathrm{salt}} r^2 \frac{\partial \overline{C}^{\mathrm{i}}_{\mathrm{salt}}}{\partial r}\right) \tag{6.1}$$

and at the membrane is (cf. (4.2))

$$\frac{\mathrm{d}R}{\mathrm{d}t} = -L_{\mathrm{p}} R_{\mathrm{gas}} T (C^{\mathrm{e}}_{\mathrm{salt}} - C^{\mathrm{i}}_{\mathrm{salt}}|_{r=R(t)}), \tag{6.2}$$

subject to the boundary conditions

$$\overline{C}^{\mathrm{i}}_{\mathrm{salt}} = \text{finite}, \quad \forall (r = 0, t), \tag{6.3}$$

and (cf. (5.1))

$$\overline{D}^{*}_{\mathrm{salt}} \frac{\partial \overline{C}^{\mathrm{i}}_{\mathrm{salt}}}{\partial r} + \frac{\mathrm{d}R}{\mathrm{d}t} C^{\mathrm{i}}_{\mathrm{salt}} = 0, \quad \forall (r = R(t), t), \tag{6.4}$$

as well as the initial conditions

$$C^{\mathrm{i}}_{\mathrm{salt}} = C^{\mathrm{i}}_{\mathrm{salt}}(0), \quad \text{at } (t = 0), \tag{6.5}$$

$$R = R_{\mathrm{i}}, \quad \text{at } (t = 0). \tag{6.6}$$

In the above equations, $C^{\mathrm{i}}_{\mathrm{salt}}$ and $\overline{C}^{\mathrm{i}}_{\mathrm{salt}}$ are related via (1.3) by

$$\overline{C}^{\mathrm{i}}_{\mathrm{salt}} = C^{\mathrm{i}}_{\mathrm{salt}} \left(1 - \frac{V_{\mathrm{b}}}{\frac{4}{3}\pi R^3}\right). \tag{6.7}$$

It seems more convenient to express the initial condition in terms of $C^{\mathrm{i}}_{\mathrm{salt}}$ as opposed to $\overline{C}^{\mathrm{i}}_{\mathrm{salt}}$ as, prior to cell expansion or contraction the cell is usually in equilibrium with a pre-initial bath concentration, and hence $C^{\mathrm{i}}_{\mathrm{salt}}(0)$ is known.

In principle, given the effective intracellular salt diffusivity $\overline{D}^{*}_{\mathrm{salt}}$, the membrane hydraulic permeability L_{p}, the external bath concentration $C^{\mathrm{e}}_{\mathrm{salt}}$, the initial cellular salt concentration $C^{\mathrm{i}}_{\mathrm{salt}}(0)$ and the initial cell radius R_{i}, the above problem enables $C^{\mathrm{i}}_{\mathrm{salt}}(r, t)$ and $R(t)$ to be calculated for all $0 \leqslant r \leqslant R$ and time t.

(*a*) *Cellular concentration distribution*

A solution to equations (6.1)–(6.7) based on a pseudo-steady state assumption is sought here. This assumption requires that the salt Peclet number, Pe_{s}, be small;

$$Pe_{\mathrm{s}} \overset{\mathrm{def}}{=} \frac{|\mathrm{d}R/\mathrm{d}t||R|}{|\overline{D}^{*}_{\mathrm{salt}}|} \ll 1. \tag{6.8}$$

This condition is easily satisfied for most cases of interest. That is, for a cell of radius $R \sim 5\,\mu\mathrm{m}$, $\overline{D}^*_{\mathrm{salt}} \sim 10^{-5}\,\mathrm{cm}^2\,\mathrm{s}^{-1}$, and a characteristic time of expansion $t \sim 10\,\mathrm{s}$, $Pe_{\mathrm{s}} \sim 3 \times 10^{-3}$. Here the symbol || refers to a suitable norm. In words, the characteristic time for the movement of the membrane is much larger than the characteristic time for diffusion of salt throughout the cell $|R|^2/|\overline{D}^*_{\mathrm{salt}}|$. In this case the differential equations uncouple, and the problem simplifies to

$$0 = \frac{1}{r^2}\frac{\partial}{\partial r}\left(\overline{D}^*_{\mathrm{salt}} r^2 \frac{\partial \overline{C}^{\mathrm{i}}_{\mathrm{salt}}}{\partial r}\right), \tag{6.9}$$

subject to

$$\overline{C}^{\mathrm{i}}_{\mathrm{salt}} = \text{finite}, \quad \forall (r = 0, t) \tag{6.10}$$

$$\overline{D}^*_{\mathrm{salt}} \frac{\partial \overline{C}^{\mathrm{i}}_{\mathrm{salt}}}{\partial r} = 0, \quad \forall (r = R, t), \tag{6.11}$$

where R is taken to be a constant. The trivial solution to this problem is that the salt concentration $\overline{C}^{\mathrm{i}}_{\mathrm{salt}}$ is constant. Invoking the fact that the number of moles of salt within the cell is conserved, we have

$$\overline{C}^{\mathrm{i}}_{\mathrm{salt}} = \frac{N_{\mathrm{salt}}}{V} = \frac{N_{\mathrm{salt}}}{\frac{4}{3}\pi R^3}, \tag{6.12}$$

or

$$C^{\mathrm{i}}_{\mathrm{salt}} = \frac{N_{\mathrm{salt}}}{\frac{4}{3}\pi R^3 - V_{\mathrm{b}}}. \tag{6.13}$$

(*b*) *Volume evolution*

Combining equations (6.2) and (6.13) yields the following equation for the size evolution of the cell:

$$\frac{\mathrm{d}R}{\mathrm{d}t} = -L_{\mathrm{p}} R_{\mathrm{gas}} T \left(C^{\mathrm{e}}_{\mathrm{salt}} - \frac{N_{\mathrm{salt}}}{\frac{4}{3}\pi R^3 - V_{\mathrm{b}}}\right), \tag{6.14}$$

subject to

$$R = R_{\mathrm{i}}, \quad \text{at } (t = 0). \tag{6.15}$$

Note that the final cell volume R_{f} can be determined by the condition $C^{\mathrm{i}}_{\mathrm{salt}} = C^{\mathrm{e}}_{\mathrm{salt}}$ as $t \to \infty$; using (6.13) this gives

$$R_{\mathrm{f}} = \left[\frac{3}{4\pi}\left(\frac{N_{\mathrm{salt}}}{C^{\mathrm{e}}_{\mathrm{salt}}} + V_{\mathrm{b}}\right)\right]^{1/3}. \tag{6.16}$$

Equation (6.14) can be solved to find $R(t)$ via a separation-of-variables technique by reformulating it as

$$\int_{R_{\mathrm{i}}}^{R} \frac{x^3}{R_{\mathrm{f}}^3 - x^3}\,\mathrm{d}x - \frac{3}{4\pi} V_{\mathrm{b}} \int_{R_{\mathrm{i}}}^{R} \frac{1}{R_{\mathrm{f}}^3 - x^3}\,\mathrm{d}x = C^{\mathrm{e}}_{\mathrm{salt}} L_{\mathrm{p}} R_{\mathrm{gas}} T t, \tag{6.17}$$

which has the solution

$$\frac{C^{\mathrm{i}}_{\mathrm{salt}}(0) L_{\mathrm{p}} R_{\mathrm{gas}} T}{R_{\mathrm{i}}} t = \frac{\eta_{\mathrm{f}}^3 - \phi_{\mathrm{i}}}{1 - \phi_{\mathrm{i}}}\left[1 - \eta + \frac{\eta_{\mathrm{f}}^3 - \phi_{\mathrm{i}}}{\eta_{\mathrm{f}}^2} F(\eta, \eta_{\mathrm{f}})\right], \tag{6.18}$$

where F is defined as

$$F(\eta,\eta_{\rm f}) \stackrel{\rm def}{=} \tfrac{1}{6}\ln\left(\frac{(\eta_{\rm f}-1)^2[(\eta_{\rm f}-\eta)^2+3\eta_{\rm f}\eta]}{(\eta_{\rm f}-\eta)^2[(\eta_{\rm f}-1)^2+3\eta_{\rm f}]}\right) + \frac{1}{\sqrt{3}}\left[\tan^{-1}\left(\frac{2\eta/\eta_{\rm f}+1}{\sqrt{3}}\right)-\tan^{-1}\left(\frac{2/\eta_{\rm f}+1}{\sqrt{3}}\right)\right], \quad (6.19)$$

along with $\eta = R/R_{\rm i}$, $\eta_{\rm f} = R_{\rm f}/R_{\rm i}$ and

$$\phi_{\rm i} = \frac{V_{\rm b}}{\frac{4}{3}\pi R_{\rm i}^3}, \quad (6.20)$$

the ratio of osmotically inactive cell volume to initial cell volume. A plot of the function $F(\eta,\eta_{\rm f})$ given in (6.19) is shown in figure 6. The actual cell volume responses of spherical cells with $\phi_{\rm i} = 0.46$ and $\phi_{\rm i} = 0.1$ (characterizing hepatocyte and erythrocyte cells) are shown in figure 7. In this figure, the responses of the two cell types (which, for the sake of the present analysis, differ only by the fraction of osmotically inactive intracellular volume) are compared against one another by fixing the total cell deformation $V_{\rm f}/V_{\rm i}$. Since the curves cross for different $\phi_{\rm i}$ at constant $V_{\rm f}/V_{\rm i}$, the dependence of the response upon $\phi_{\rm i}$ is not one of simply scaling a characteristic curve. On the other hand, each of these two cell types will in general have different membrane hydraulic permeabilities $L_{\rm p}$ and initial radii $R_{\rm i}$; these, however, only enter into the time variable and not explicitly into the curves, meaning that the cells are self-similar in this respect. In other words, once $\eta_{\rm f}$ and $\phi_{\rm i}$ are known, there is only one curve describing the osmotic response independent of the choice of $L_{\rm p}$ or $R_{\rm i}$ (or any of the other scaled variables). Whereas figure 7 compares the response keeping $V_{\rm f}/V_{\rm i}$ constant, one could also compare the two by keeping the ratio $C^{\rm e}_{\rm salt}/C^{\rm i}_{\rm salt}(0)$ fixed. The two are related by (cf. (6.13) and (6.16))

$$\frac{C^{\rm e}_{\rm salt}}{C^{\rm i}_{\rm salt}(0)} = \frac{1-\phi_{\rm i}}{\eta_{\rm f}^3-\phi_{\rm i}}. \quad (6.21)$$

In figure 7, $\eta_{\rm f}$ was fixed while figure 8 shows the response of the two cell types upon either doubling or halving the external salt concentration. A smaller inactive volume fraction $\phi_{\rm i}$ gives rise to a larger osmotic response.

(c) *Hydraulic permeability* $L_{\rm p}$

The curves shown in figure 8 suggest a possible protocol for measuring the hydraulic permeability $L_{\rm p}$. If cells are subjected to hyposmotic conditions, say $C^{\rm e}_{\rm salt}/C^{\rm i}_{\rm salt}(0) = \frac{1}{2}$ and the time taken for the cell to undergo half its volume expansion $t_{1/2}$ is measured, then $L_{\rm p}$ could be determined from (6.18) directly. For the case of hepatocytes this halftime would be related to $L_{\rm p}$ by

$$L_{\rm p} = \frac{0.290R_{\rm i}}{C^{\rm i}_{\rm salt}(0)R_{\rm gas}Tt_{1/2}}, \quad \forall\left(\phi_{\rm i}=0.46,\ \frac{C^{\rm e}_{\rm salt}}{C^{\rm i}_{\rm salt}(0)}=\tfrac{1}{2}\right), \quad (6.22)$$

while for erythrocytes $L_{\rm p}$ could be determined from

$$L_{\rm p} = \frac{0.457R_{\rm i}}{C^{\rm i}_{\rm salt}(0)R_{\rm gas}Tt_{1/2}}, \quad \forall\left(\phi_{\rm i}=0.1,\ \frac{C^{\rm e}_{\rm salt}}{C^{\rm i}_{\rm salt}(0)}=\tfrac{1}{2}\right). \quad (6.23)$$

The coefficients 0.290 and 0.457 are functions of $\phi_{\rm i}$ and $C^{\rm e}_{\rm salt}/C^{\rm i}_{\rm salt}(0)$. They can be determined by first calculating $\eta_{\rm f}$ from (6.21) and combining this with $\eta^3 =$

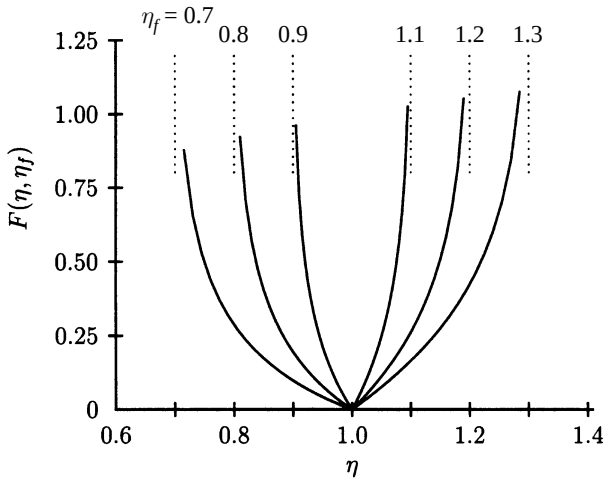

Figure 6. Graph of $F(\eta, \eta_f)$ as a function of $\eta = R/R_i$ and $\eta_f = R_f/R_i$. The extreme values $\eta_f = 0.7$ and $\eta_f = 1.3$ correspond to volume changes of $V_f/V_i \simeq 0.34$ and $V_f/V_i \simeq 2.2$, respectively. The function has asymptotes at $\eta = \eta_f$.

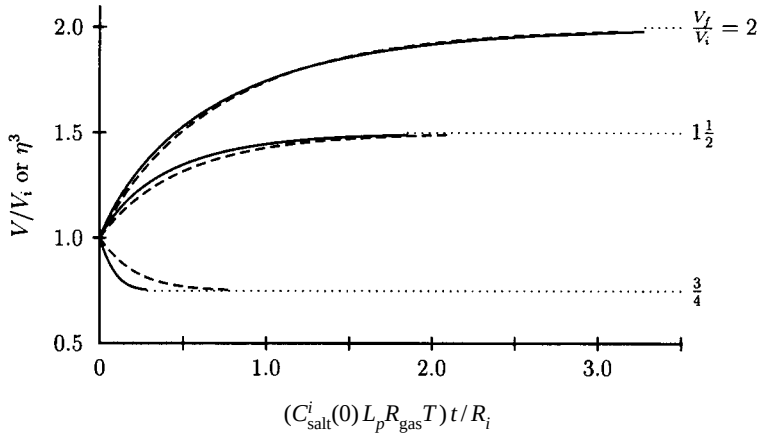

Figure 7. Response of hepatocytes and erythrocytes to osmotic stress caused by varying the external salt concentration such that the change in volume V_f/V_i is constant. The end point of each curve corresponds to the cell completing 98% of its response.

$\eta^3_{1/2} = \frac{1}{2}(\eta_f^3 + 1)$ in equations (6.18) and (6.19). Note that $\eta_{1/2}$ denotes the radius corresponding to the cell volume $V_{1/2} = V_i + \frac{1}{2}(V_f - V_i)$, not to the midpoint value of the radius.

(*d*) *Boyle van't Hoff relationship*

Finally, consider the case where, prior to setting the external bath concentration to C^e, the bath is isosmotic C^e_{iso}†. This means that initially the internal cell concentration is simply $C^i_{salt}(0) = C^e_{iso}$ and the cell has volume V_{iso}. The final cell volume V assumed by the cell upon equilibriating with the bath concentration C^e can be

† The salt subscript has been dropped in this subsection since this analysis is restricted to the salt case.

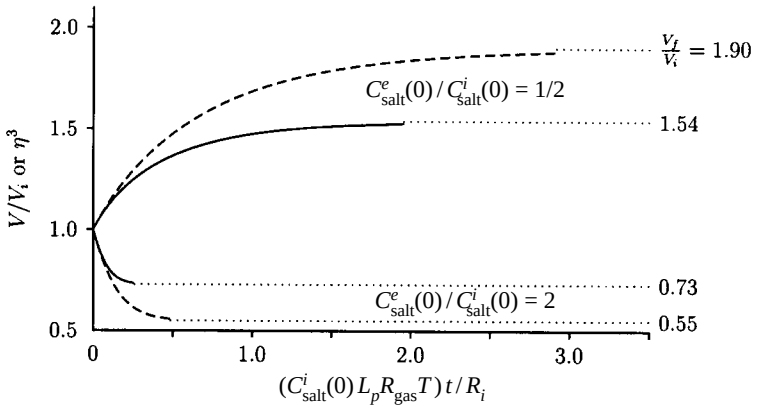

Figure 8. Response of hepatocytes and erythrocytes to osmotic stress caused by either doubling or halfing the external salt concentration. Curve endpoints correspond to 98% response.

obtained directly from (6.21) and is conveniently written as

$$\frac{V}{V_{\rm iso}} = \frac{C^{\rm e}_{\rm iso}}{C^{\rm e}}\left(1 - \frac{V_{\rm b}}{V_{\rm iso}}\right) + \frac{V_{\rm b}}{V_{\rm iso}}. \tag{6.24}$$

This is the classical Boyle van't Hoff relationship. Given the isosmotic cell parameters $V_{\rm iso}$ and $C^{\rm e}_{\rm iso}$, the cell is stressed to a new condition characterized by V and $C^{\rm e}$. Equation (6.24) then allows for the determination of the osmotically inactive cell volume $V_{\rm b}$ by equilibrium measurements of V versus $C^{\rm e}$.

7. Salt and semipermeable solute response

In the presence of semipermeable solute, the osmotic response of a cell due to unequal internal and external salt and semipermeable solute concentrations is governed by (6.1) and

$$\frac{\partial \overline{C}^{\rm i}_{\rm sp}}{\partial t} = \frac{1}{r^2}\frac{\partial}{\partial r}\left(\overline{D}^*_{\rm sp} r^2 \frac{\partial \overline{C}^{\rm i}_{\rm sp}}{\partial r}\right), \tag{7.1}$$

$$\frac{{\rm d}R}{{\rm d}t} = -L_{\rm p}R_{\rm gas}T[(C^{\rm e}_{\rm salt} - C^{\rm i}_{\rm salt}|_{r=R(t)}) + \sigma(C^{\rm e}_{\rm sp} - C^{\rm i}_{\rm sp}|_{r=R(t)})] \tag{7.2}$$

subject to the boundary conditions (6.3), (6.4) and

$$\overline{C}^{\rm i}_{\rm sp} = \text{finite}, \quad \forall (r = 0, t), \tag{7.3}$$

$$\overline{D}^*_{\rm sp}\frac{\partial \overline{C}^{\rm i}_{\rm sp}}{\partial r} + \frac{{\rm d}R}{{\rm d}t}C^{\rm i}_{\rm sp} = P_{\rm sp}(C^{\rm e}_{\rm sp} - C^{\rm i}_{\rm sp}), \quad \forall (r = R(t), t) \tag{7.4}$$

the initial conditions (6.5) and

$$C^{\rm i}_{\rm sp} = C^{\rm i}_{\rm sp}(0), \quad \text{at } (t = 0) \tag{7.5}$$

$$R = R_{\rm i}, \quad \text{at } (t = 0). \tag{7.6}$$

and the relations (6.7) and

$$\overline{C}^{\rm i}_{\rm sp} = C^{\rm i}_{\rm sp}(1 - \phi + k\alpha + K\phi), \quad \forall (r, t), \tag{7.7}$$

where, of course, the osmotically inactive volume fraction ϕ is a function of R. This problem is well defined, and, in principal, given the properties of the bath ($C^{\rm e}_{\rm sp}$,

$C^{\mathrm{e}}_{\mathrm{salt}}$), cytosol ($\overline{D}^{*}_{\mathrm{sp}}$, $\overline{D}^{*}_{\mathrm{salt}}$), membrane ($L_{\mathrm{p}}$, σ, P_{sp}) and initial data ($C^{\mathrm{i}}_{\mathrm{sp}}(0)$, $C^{\mathrm{i}}_{\mathrm{salt}}(0)$, R_{i}), the resulting fields $\overline{C}^{\mathrm{i}}_{\mathrm{sp}}(r,t)$, $\overline{C}^{\mathrm{i}}_{\mathrm{salt}}(r,t)$ and $R(t)$ can be determined. The amount of semipermeable solute within the cell $N_{\mathrm{sp}}(t)$ can then be determined from

$$N_{\mathrm{sp}}(t) = 4\pi \int_0^{R(t)} \overline{C}^{\mathrm{i}}_{\mathrm{sp}}(r,t) r^2 \,\mathrm{d}r. \tag{7.8}$$

Once again, because of the nonlinear nature of the boundary conditions, (6.4) and (7.4), determining an exact solution is non-trivial.

(*a*) *Cellular concentration distribution*

As in the case of pure salt transport, addressed in § 6, a pseudo-steady state assumption is generally appropriate and can be used to simplify the problem. It is required that both the *salt* Peclet number (6.8) and the *semipermeable solute* Peclet number be small. The latter requires

$$Pe_{\mathrm{s}} \overset{\mathrm{def}}{=} \frac{|\mathrm{d}R/\mathrm{d}t||R|}{|\overline{D}^{*}_{\mathrm{sp}}|} \ll 1. \tag{7.9}$$

This is equivalent to assuming that both salt and semipermeable solute diffuse throughout the cell on a much shorter time scale than that associated with the movement of the cell membrane. This leads to an uncoupling of the concentration and radial evolution problems. The concentration problems may then be solved first. It is important to note that, although (7.9) holds in most physical problems of interest (see the discussion following (6.8)), an additional time scale is introduced in the problem under consideration owing to the permeability P_{sp} of the membrane to the semipermeable solute. Since the rate of semipermeable solute entry into the cell is characterized by P_{sp}, the relevant Peclet number characterizing the diffusion equation is

$$Pe = \frac{P_{\mathrm{sp}} R}{\overline{D}^{*}_{\mathrm{sp}}}, \tag{7.10}$$

which is, in general, finite. In any case, it is not permissible to neglect the time derivative in (7.1) as, even if $Pe \ll 1$, a physically important concentration gradient (however small) will exist inside the cell, such that diffusion *across* the membrane balances diffusion *to* the membrane and unsteady behaviour is realized.

The equations governing the evolution of the salt concentration are identical to those derived in the absence of semipermeable solute (6.9)–(6.11). As such, the salt concentration is found to be independent of r and given by

$$C^{\mathrm{i}}_{\mathrm{salt}} = \frac{N_{\mathrm{salt}}}{\frac{4}{3}\pi R^3 - V_{\mathrm{b}}}. \tag{7.11}$$

In this pseudo-steady state limit, ϕ appears to be constant and independent of time. As such, it is easiest to work with $C^{\mathrm{i}}_{\mathrm{sp}}$ (as opposed to $\overline{C}^{\mathrm{i}}_{\mathrm{sp}}$), where the equations governing the semipermeable solute concentration $C^{\mathrm{i}}_{\mathrm{sp}}$ become

$$\frac{\partial C^{\mathrm{i}}_{\mathrm{sp}}}{\partial t} = \frac{1}{r^2}\frac{\partial}{\partial r}\left(\overline{D}^{*}_{\mathrm{sp}} r^2 \frac{\partial C^{\mathrm{i}}_{\mathrm{sp}}}{\partial r}\right), \tag{7.12}$$

subject to

$$C^{\mathrm{i}}_{\mathrm{sp}} = \text{finite}, \quad \forall (r = 0, t), \tag{7.13}$$

$$\overline{D}^{*}_{\mathrm{sp}}(1-\phi+k\alpha+K\phi)\frac{\partial C^{\mathrm{i}}_{\mathrm{sp}}}{\partial r}=P_{\mathrm{sp}}(C^{\mathrm{e}}_{\mathrm{sp}}-C^{\mathrm{i}}_{\mathrm{sp}}),\quad \forall(r=R,t) \tag{7.14}$$

and

$$C^{\mathrm{i}}_{\mathrm{sp}}=C^{\mathrm{i}}_{\mathrm{sp}}(0),\quad \text{at } (t=0), \tag{7.15}$$

with R taken to be a constant. In the most general case, the semipermeable solute diffusivity $\overline{D}^{*}_{\mathrm{sp}}$ may be a function of (among other variables) the osmotically inactive volume fraction ϕ; however, since this pseudo-steady state analysis is akin to assuming that R, and hence ϕ, is constant with respect to semipermeable solute diffusion within the cell, $\overline{D}^{*}_{\mathrm{sp}}$ appears to be a constant when solving for the semipermeable solute field $C^{\mathrm{i}}_{\mathrm{sp}}$.

Momentarily ignoring the initial condition, (7.15), the solution $C^{\mathrm{i}}_{\mathrm{sp}}(r,t)$ may be determined by assuming a separation-of-variables type solution of the form $C^{\mathrm{i}}_{\mathrm{sp}}(r,t)=f(r)g(t)$. The general solution of (7.12)–(7.14) then is

$$C^{\mathrm{i}}_{\mathrm{sp}}(r,t)=C^{\mathrm{e}}_{\mathrm{sp}}+\sum_{n=1}^{\infty}A_n\frac{\sin(\lambda_n r/R)}{r/R}\mathrm{e}^{-\lambda_n^2\overline{D}^{*}_{\mathrm{sp}}t/R^2}, \tag{7.16}$$

where the eigenvalues λ_n are taken to be the non-zero roots of the transendential equation

$$\beta\lambda_n=\tan(\lambda_n), \tag{7.17}$$

with the coefficient β defined as

$$\beta\overset{\mathrm{def}}{=}\left(1-\frac{P_{\mathrm{sp}}R}{\overline{D}^{*}_{\mathrm{sp}}(1-\phi+k\alpha+K\phi)}\right)^{-1}. \tag{7.18}$$

Note that while λ_n are essentially constant over the (rapid) time scale of diffusion they (slowly) change in time over the time scale of cell membrane expansion (cf. (7.35)–(7.37)). Given the low Peclet conditions, in the derivation of (7.16), λ_n are taken to be time constants. The values of λ_n for various values of $P_{\mathrm{sp}}R/[\overline{D}^{*}_{\mathrm{sp}}(1-\phi+k\alpha+K\phi)]$ are given in table 1. Since (7.17) is analytic, a Newton–Rhapson method combined with a bisection method (used to keep the root bound and to guarantee at least linear convergence) was used to calculate the eigenvalues (Press *et al.* 1994). A useful property in computing these roots is that they are bound by the inequality

$$(n-1)\pi<\lambda_n<n\pi,\quad \forall\left(0<\frac{P_{\mathrm{sp}}R}{\overline{D}^{*}_{\mathrm{sp}}(1-\phi+k\alpha+K\phi)}<\infty,\ n\geqslant 1\right). \tag{7.19}$$

Roots of (7.17) may also be found in other standard texts (Abramowitz & Stegun 1972). The coefficients A_n appearing in (7.16) can be determined from the initial condition, (7.15). Set $t=0$ in (7.16), multiply by the function $r\sin(\lambda_{\mathrm{m}}r/R)$, integrate over r and use the orthogonality properties of the eigenfunctions to obtain

$$A_n=[C^{\mathrm{i}}_{\mathrm{sp}}(0)-C^{\mathrm{e}}_{\mathrm{sp}}]\frac{2}{\lambda_n}\frac{\sin(\lambda_n)-\lambda_n\cos(\lambda_n)}{\lambda_n-\sin(\lambda_n)\cos(\lambda_n)}. \tag{7.20}$$

The above is equivalent to the pure salt problem considered in § 6 when $P_{\mathrm{sp}}=0$. In this case the eigenvalues satisfy $\lambda_n=\tan(\lambda_n)$ resulting in the coefficients all being identically zero, $A_n=0$. As such, the erroneous result obtains $C^{\mathrm{i}}_{\mathrm{sp}}(r,t)=C^{\mathrm{e}}_{\mathrm{sp}}$. This is purely a consequence of the singular nature of the condition $P_{\mathrm{sp}}=0$ because for all $P_{\mathrm{sp}}>0$ no matter how infinitely small, the semipermeable solute will eventually either leave or enter the cell so as to equilibriate with $C^{\mathrm{e}}_{\mathrm{sp}}$.

Table 1. *The first five eigenvalues λ_n for various values of $P_{\rm sp}R/[\overline{D}^*_{\rm sp}(1-\phi+k\alpha+K\phi)]$*

$\frac{P_{\rm sp}R}{\overline{D}^*_{\rm sp}(1-\phi+k\alpha+K\phi)}$	λ_1	λ_2	λ_3	λ_4	λ_5
0	0	4.493 41	7.725 25	10.9041	14.0662
0.001	0.054 7668	4.493 63	7.725 38	10.9042	14.0663
0.01	0.173 032	4.495 63	7.726 55	10.9050	14.0669
0.1	0.542 281	4.515 66	7.738 20	10.9133	14.0733
0.5	1.165 56	4.604 22	7.789 88	10.9499	14.1017
0.9	1.504 42	4.691 08	7.841 23	10.9865	14.1301
1	$\pi/2$	$3\pi/2$	$5\pi/2$	$7\pi/2$	$9\pi/2$
2	2.028 76	4.913 18	7.978 67	11.0855	14.2074
5	2.570 43	5.354 03	8.302 93	11.3348	14.4080
10	2.836 30	5.717 25	8.658 70	11.6532	14.6869
100	3.110 18	6.220 44	9.330 81	12.4414	15.5214
1000	3.138 45	6.276 90	9.415 35	12.5538	15.6923
∞	π	2π	3π	4π	5π

Finally, the semipermeable solute concentration at the membrane $r = R$ is given by

$$C^{\rm i}_{\rm sp}(R,t) = C^{\rm e}_{\rm sp} + [C^{\rm i}_{\rm sp}(0) - C^{\rm e}_{\rm sp}]2\sum_{n=1}^{\infty} \frac{\sin^2(\lambda_n) - \lambda_n \sin(\lambda_n)\cos(\lambda_n)}{\lambda_n^2 - \lambda_n \sin(\lambda_n)\cos(\lambda_n)} {\rm e}^{-\lambda_n^2 \overline{D}^*_{\rm sp} t/R^2}. \tag{7.21}$$

(*b*) *Volume evolution*

Direct substitution of the expressions for the salt (7.11) and semipermeable solute (7.21) concentrations at the membrane into the evolution equation (7.2) yields

$$-\frac{1}{L_{\rm p}R_{\rm gas}T}\frac{{\rm d}R}{{\rm d}t} = C^{\rm e}_{\rm salt} - \frac{N_{\rm salt}}{\frac{4}{3}\pi R^3 - V_{\rm b}} + \sigma[C^{\rm e}_{\rm sp} - C^{\rm i}_{\rm sp}(0)]2\sum_{n=1}^{\infty} \frac{\sin^2(\lambda_n) - \lambda_n \sin(\lambda_n)\cos(\lambda_n)}{\lambda_n^2 - \lambda_n \sin(\lambda_n)\cos(\lambda_n)} {\rm e}^{-\lambda_n^2 \overline{D}^*_{\rm sp} t/R^2}, \tag{7.22}$$

subject to the initial condition

$$R = R_{\rm i}, \quad \text{at } (t = 0). \tag{7.23}$$

As in the salt case, greater clarity of the problem is provided upon converting to dimensionless variables. To this end, define the characteristic time scale for water diffusion across the cell membrane as

$$t_{\rm w} \stackrel{\rm def}{=} \frac{R_{\rm i}}{C^{\rm i}_{\rm salt}(0) L_{\rm p} R_{\rm gas} T}, \tag{7.24}$$

the characteristic time scale for semipermeable solute diffusion across the cell membrane as

$$t_{\mathrm{sp}} \stackrel{\mathrm{def}}{=} \frac{R_{\mathrm{i}}}{P_{\mathrm{sp}}}, \tag{7.25}$$

the salt driving force as

$$\delta_{\mathrm{salt}} \stackrel{\mathrm{def}}{=} \frac{C^{\mathrm{e}}_{\mathrm{salt}}}{C^{\mathrm{i}}_{\mathrm{salt}}(0)} \tag{7.26}$$

and the semipermeable solute driving force as

$$\delta_{\mathrm{sp}} \stackrel{\mathrm{def}}{=} \sigma \frac{C^{\mathrm{i}}_{\mathrm{sp}}(0) - C^{\mathrm{e}}_{\mathrm{sp}}}{C^{\mathrm{i}}_{\mathrm{salt}}(0)}. \tag{7.27}$$

Rewriting (7.22) in terms of $\tau = t/t_{\mathrm{w}}$, $\eta = R/R_{\mathrm{i}}$ and these defined parameters; we have

$$\frac{\mathrm{d}\eta}{\mathrm{d}\tau} = \frac{1-\phi_{\mathrm{i}}}{\eta^3 - \phi_{\mathrm{i}}} - \delta_{\mathrm{salt}} + \delta_{\mathrm{sp}} 2 \sum_{n=1}^{\infty} \frac{\sin^2(\lambda_n) - \lambda_n \sin(\lambda_n)\cos(\lambda_n)}{\lambda_n^2 - \lambda_n \sin(\lambda_n)\cos(\lambda_n)} \mathrm{e}^{-\lambda_n^2 (\overline{D}^*_{\mathrm{sp}} t_{\mathrm{w}}/R_{\mathrm{i}}^2)(\tau/\eta^2)}, \tag{7.28}$$

$$\eta = 1, \quad \text{at } (\tau = 0), \tag{7.29}$$

along with the eigenvalues representing the non-zero roots of

$$\frac{\lambda_n}{1 - \dfrac{R_{\mathrm{i}}^2}{t_{\mathrm{sp}} \overline{D}^*_{\mathrm{sp}} (1 - \phi + k\alpha + K\phi)} \eta} = \tan(\lambda_n), \tag{7.30}$$

and the fact that ϕ is related to η by $\phi = \phi_{\mathrm{i}}/\eta^3$. An important observation is that the semipermeable solute does not influence the final cell radius R_{f}. This can be seen explicitly in (7.28) where, since the membrane is permeable to the semipermeable solute, the transient terms vanish at long time. The final cell radius can then be calculated exactly, as in the salt-only case, from (6.16).

(*c*) *Effective semipermeable solute diffusivity*

Solution of (7.28)–(7.30) requires knowledge of the effective diffusivity, $\overline{D}^*_{\mathrm{sp}}$. In general, this effective diffusion coefficient will *not* be equivalent to the cytosolic (i.e. water) diffusivity $D^{\mathrm{cyt}}_{\mathrm{sp}}$. The reason for this is that the semipermeable solute may tend to absorb into internal organelle membranes, where it displays a lateral membrane diffusivity, $D^{\mathrm{surf}}_{\mathrm{sp}}$ (Clegg & Vaz 1985). As has already been discussed in § 1, the absorption of semipermeable solute to internal organelle membranes can be characterized by the Henry's law absorption coefficient, k. Given that the solute, during its passage through the cytosol, will spend a certain amount of time absorbed to organelle membranes, the effective diffusivity $\overline{D}^*_{\mathrm{sp}} \neq D^{\mathrm{cyt}}_{\mathrm{sp}}$. An explicit expression for the effective diffusivity exists in the special case (considered here) where the internal cell organelles are spherical and of identical radius, a. This assumption implies that the specific surface area, α, is given as

$$\alpha = 3\phi/a. \tag{7.31}$$

In this case, accounting for semipermeable solute absorption onto the membranes of internal cell organelles, the semipermeable solute diffusivity has the form (Edwards

& Davis 1995)

$$\overline{D}^{*}_{\mathrm{sp}} = \frac{D^{\mathrm{cyt}}_{\mathrm{sp}}}{1-\phi+k\alpha+K\phi}\left[1-\frac{3\phi(1-K)}{2+K+2\Gamma+\phi(1-K-2\Gamma)+\mathcal{O}(\phi^{10/3})}\right], \quad (7.32)$$

where $D^{\mathrm{cyt}}_{\mathrm{sp}}$ is the semipermeable solute diffusivity in the cytosol and Γ is defined as

$$\Gamma \stackrel{\mathrm{def}}{=} k\frac{D^{\mathrm{surf}}_{\mathrm{sp}}}{aD^{\mathrm{cyt}}_{\mathrm{sp}}}, \quad (7.33)$$

with $D^{\mathrm{surf}}_{\mathrm{sp}}$ the surface diffusivity of the semipermeable solute on the organelle membranes. The form of $\overline{D}^{*}_{\mathrm{sp}}$ allows for the identification of another relevant time scale, namely, the characteristic time associated with diffusion of the semipermeable solute to the cell membrane through the cytosol. This time scale is defined as

$$t^{\mathrm{cyt}}_{\mathrm{sp}} \stackrel{\mathrm{def}}{=} \frac{R^2_{\mathrm{i}}}{D^{\mathrm{cyt}}_{\mathrm{sp}}}. \quad (7.34)$$

The evolution of the cell radius (7.28) then takes on the form

$$\frac{\mathrm{d}\eta}{\mathrm{d}\tau} = \frac{1-\phi_{\mathrm{i}}}{\eta^3-\phi_{\mathrm{i}}} - \delta_{\mathrm{salt}} + \delta_{\mathrm{sp}} 2\sum_{n=1}^{\infty}\frac{\sin^2(\lambda_n)-\lambda_n\sin(\lambda_n)\cos(\lambda_n)}{\lambda_n^2-\lambda_n\sin(\lambda_n)\cos(\lambda_n)}\mathrm{e}^{-\lambda_n^2\tau_{\mathrm{w}}(\overline{D}^{*}_{\mathrm{sp}}/D^{\mathrm{cyt}}_{\mathrm{sp}})(\tau/\eta^2)}, \quad (7.35)$$

$$\eta = 1, \quad \text{at } (\tau = 0), \quad (7.36)$$

along with the eigenvalues representing the non-zero roots of

$$\frac{\lambda_n}{1-\dfrac{1}{\tau_{\mathrm{sp}}(1-\phi+k\alpha+K\phi)}\dfrac{D^{\mathrm{cyt}}_{\mathrm{sp}}}{\overline{D}^{*}_{\mathrm{sp}}}\eta} = \tan(\lambda_n), \quad (7.37)$$

where the dimensionless time scales $\tau_{\mathrm{w}} = t_{\mathrm{w}}/t^{\mathrm{cyt}}_{\mathrm{sp}}$ and $\tau_{\mathrm{sp}} = t_{\mathrm{sp}}/t^{\mathrm{cyt}}_{\mathrm{sp}}$ represent the respective ratios of water and semipermeable solute diffusion time scales across the membrane relative to the semipermeable solute diffusion time scale within the cytosol. These coefficients are expected to be large in accordance with the pseudo-steady state hypothesis.

Strictly speaking, this volume evolution $\eta(\tau)$ depends upon (at most) *eight* dimensionless constants;

$$\eta = \eta\left(\tau\middle|\phi_{\mathrm{i}}, \delta_{\mathrm{salt}}, \delta_{\mathrm{sp}}, \tau_{\mathrm{w}}, \tau_{\mathrm{sp}}, \frac{k}{a}, K, \frac{D^{\mathrm{surf}}_{\mathrm{sp}}}{D^{\mathrm{cyt}}_{\mathrm{sp}}}\right). \quad (7.38)$$

Since (7.32) and (7.35) are quite complicated, analytical evaluation is difficult. Note also that the eigenvalues (7.37) depend upon $R(t)$, so are themselves changing in time. Furthermore, the semipermeable solute diffusivity $\overline{D}^{*}_{\mathrm{sp}}$ is a function of the instantaneous osmotically inactive volume fraction ϕ, itself a function of $R(t)$. As such, (7.32) and (7.35) have been analysed numerically in the present study. All volume responses have been calculated using a Cash–Karp Runge–Kutta integration scheme (Press *et al.* 1994). This algorithm takes fifth order Runge–Kutta steps where each step size is adjusted so as to bound the fractional errors in η by a specified value.

(*d*) *Predicting kinetic volume changes: hepatocyte base case*

Recapitulating, the main results of this article are those of (6.18) (and its equilibrium corollary (6.24)) and (7.35)–(7.37). The former describes the cell volume

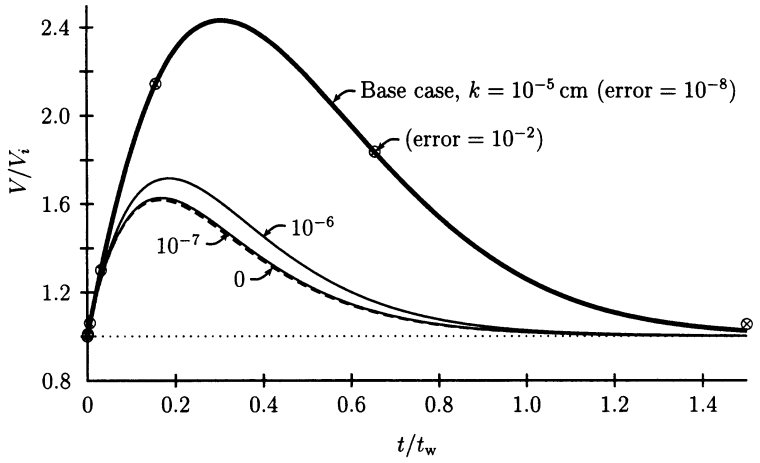

Figure 9. Hepatocyte response during removal of a semipermeable solute. All other things being equal, the effect of varying k/a is shown. The dashed line represents the response when absorption is assumed to be absent $k = 0$. Also shown is the computed base case when a relative error of 10^{-2} is enforced.

changes caused by anisosmotic salt conditions (see figures 7 and 8) whereas the latter describes the volume kinetics caused by a disequilibrium in semipermeable solute concentrations.

The semipermeable solute disequilibrium problem is considerably more rich than the salt-only problem, primarily owing to the preponderance of transport mechanisms in the former case. In this section, we consider in detail the solution of (7.35)–(7.37) using a 'base case' corresponding to the *thawing cycle of a hepatocyte* (as depicted qualitatively in figure 2).

The relevant hepatocyte parameters are listed in table 2. In this table, the internal organelle radius, a, has been chosen to accurately reflect the amount of internal membrane to which the semipermeable solute can absorb. For a hepatocyte, the total amount of membrane is roughly comprised of 98% internal (Alberts *et al.* 1994); given that the hepatocyte volume is approximately 5000 μm^3, this means the internal membrane area is approximately 69 288 μm^2. Distributing the total organelle membrane area over the total inactive cell volume, and requiring organelles to be of identical radius, a, gives $a = 100$ nm. The Henry's law absorption coefficient k, scales like the thickness of a characteristic organelle membrane times the relative partitioning of the semipermeable solute into the membrane. Assuming the organelle membrane thickness is about 10 nm and the semipermeable solute partitions 10 fold into the membranes gives $k = 100$ nm, which is the value appearing in table 2. The values of other variables, such as P_{sp} and L_p, correspond to characteristic values (Gilmore *et al.* 1996) for a range of cryoprotectant and cell types.

The 'base case' (table 2) response along with its dependence upon absorption is shown in figure 9. The cell undergoes a peak volume expansion of roughly 140%, a value at which the cell might indeed lyse—an eventuality that can be easily included into the analysis, though we have not done so here. Absorption has a pronounced effect on the volume response. Hence, the 'apparent' values of P_{sp} and L_p depend markedly on absorption. This is further discussed in the next subsection, where a definitive way of measuring P_{sp} and L_p from the volume response is addressed.

Figure 9 also shows the accuracy of the Cash–Karp Runge–Kutta integration scheme used to compute the response. The fractional error at each point is defined

Table 2. *Hepatocyte: base case*

(Characteristic values of the relevant parameters for a hepatocyte. This 'base case' corresponds to removing the cryoprotectant from the cell in isosmotic salt conditions. The dimensionless response $\eta(\tau)$ is unique given the last eight coefficients in the table.)

symbol	value	units
T	22	°C
V_{i}	5000	$\mu\mathrm{m}^3$
V_{b}	2300	$\mu\mathrm{m}^3$
σ	0.9	—
$D_{\mathrm{sp}}^{\mathrm{cyt}}$	10^{-6}	$\mathrm{cm}^2\ \mathrm{s}^{-1}$
$D_{\mathrm{sp}}^{\mathrm{surf}}$	10^{-7}	$\mathrm{cm}^2\ \mathrm{s}^{-1}$
K	0	—
a	10^{-5}	cm
k	10^{-5}	cm
L_{p}	1.0	$\mu\mathrm{m\ min}^{-1}\ \mathrm{atm}^{-1}$
P_{sp}	0.002	$\mathrm{cm\ min}^{-1}$
$C_{\mathrm{salt}}^{\mathrm{i}}(0)$	0.26	$\mathrm{mol\ l}^{-1}$
$C_{\mathrm{salt}}^{\mathrm{e}}$	0.26	$\mathrm{mol\ l}^{-1}$
$C_{\mathrm{sp}}^{\mathrm{i}}(0)$	1.0	$\mathrm{mol\ l}^{-1}$
$C_{\mathrm{sp}}^{\mathrm{e}}$	0	$\mathrm{mol\ l}^{-1}$
R_{i}	10.6	$\mu\mathrm{m}$
t_{w}	101	s
t_{sp}	31.8	s
$t_{\mathrm{sp}}^{\mathrm{cyt}}$	1.13	s
ϕ_{i}	0.46	—
δ_{salt}	1	—
δ_{sp}	3.46	—
τ_{w}	89.8	—
τ_{sp}	28.3	—
K	0	—
k/a	1	—
$D_{\mathrm{sp}}^{\mathrm{surf}}/D_{\mathrm{sp}}^{\mathrm{cyt}}$	0.1	—

as the difference between the fifth- and fourth-order Runge–Kutta estimations of η computed at a point $n+1$ and normalized by the fifth-order η computed at the previous step n. The step size is adjusted to bound this error at each step by a specified value. The accuracy of the solution with an error as large as 10^{-2} requires only six steps across the domain and gives values which are very close to convergence using an error of 10^{-8}.

If, prior to removing the semipermeable solute from the cell (as in figure 9), the cell was immersed in a solution of salt and semipermeable solute, the response shown in figure 10 would follow. (The only difference between this case and the base case is a change of sign of δ_{sp}, where now the initial semipermeable solute concentration $C_{\mathrm{sp}}^{\mathrm{i}}(0)$ inside the cell is zero, while the external solute concentration $C_{\mathrm{sp}}^{\mathrm{e}}$ is held at $1\ \mathrm{mol\ l}^{-1}$.) Also shown is the effect of internal membrane absorption.

Figure 11 shows the sensitivity of the response of the base case due to a change in the semipermeable solute permeability P_{sp}, while figure 12 shows the sensitivity due to a change in the hydraulic permeability L_{p}. In terms of the seven dimensionless

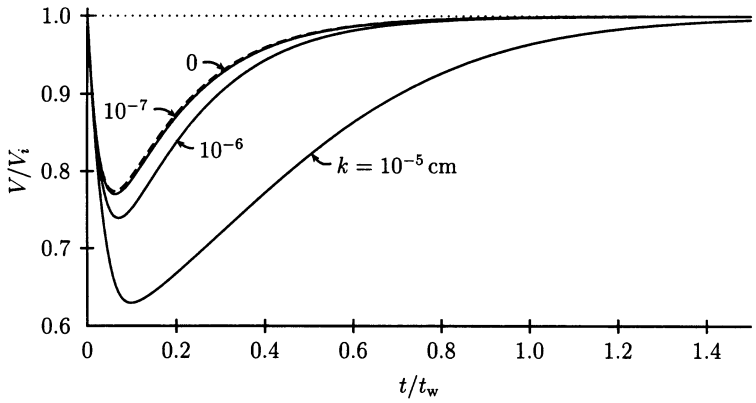

Figure 10. Hepatocyte response during loading of a semipermeable solute. The difference from the base case data is a switch in the sign of the semipermeable solute driving force, $\delta_{sp} = -3.46$. All other things being equal, the effect of varying k/a is shown.

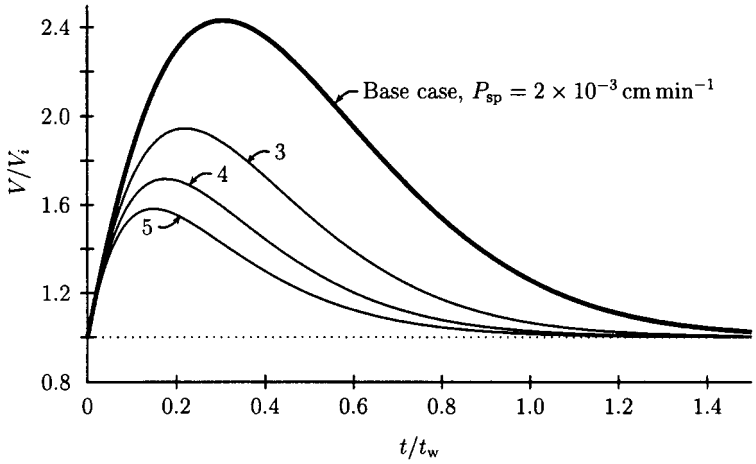

Figure 11. Hepatocyte response during removal of a semipermeable solute. All other things being equal, the effect of varying τ_{sp} is shown.

variables, the former represents a change in τ_{sp} while the latter a change in τ_w. The magnitude of the peak decreases as P_{sp} is increased or L_p is decreased. Furthermore, the dimensionless time at which the peak occurs is lessened with this adjustment of P_{sp} or L_p. Importantly, in figure 12, since L_p is changing, t_w *is also changing*, and, as such, the true time, t, at which the peak occurs is actually increasing with decreasing L_p. These last two figures highlight the importance of including membrane absorption in the interpretation of results, for a 50% volume expansion might, lacking an unequivocal way of determining parameters, be attributed to either: (i) lower absorption; (ii) larger P_{sp}; or (iii) smaller L_p.

(*e*) *Experimental protocol for the determination of* k, P_{sp} *and* L_p

The practical utility of the preceeding results is that they can be directly used to interpret 'osmotic-challenge' experiments, and thereby used to deduce membrane transport parameters in an unequivocal fasion.

In this subsection, a protocol is outlined, based upon the above, allowing the direct

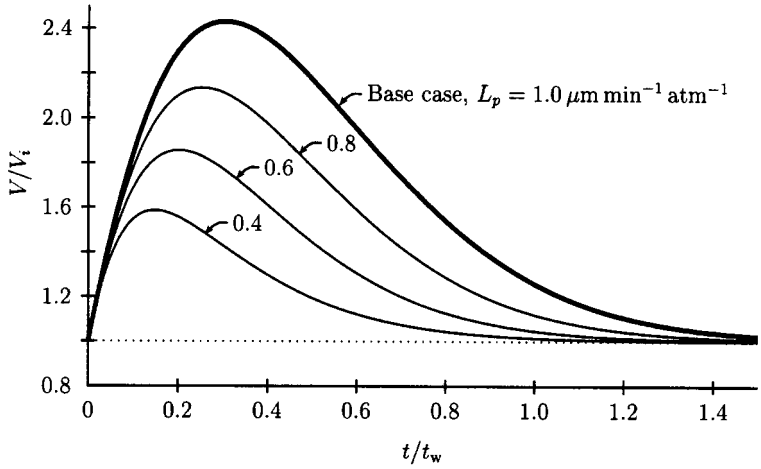

Figure 12. Hepatocyte response during removal of a semipermeable solute. All other things being equal, the effect of varying τ_{w} is shown. Also, the characteristic water time t_{w} changes from 101 s to 253 s as L_{p} varies from 1.0 to 0.4.

determination of P_{sp} and L_{p} from experimental measurements of the cell volume response to a homogeneous osmotic imbalance.

First, we note that the adsorption parameter, k, can be obtained by equilibrium measurements. It follows directly from (1.4), (1.6) and (7.31) that, in the presence of a semipermeable solute and at equilibrium, the amount of semipermeable solute within the cell is related to the external bath concentration by

$$\frac{N_{\mathrm{sp}}}{V} = C^{\mathrm{e}}_{\mathrm{sp}} \left(1 - \phi + 3\phi \frac{k}{a} + K\phi\right). \tag{7.39}$$

Since N_{sp}, V, ϕ, K and $C^{\mathrm{e}}_{\mathrm{sp}}$ are all known or measurable, (7.39) allows for the the determination of k/a directly from the equilibrium state of the cell.

Consider the cell to contain semipermeable solute and to be immersed in an isosmotic bath that, at least initially, contains no semipermeable solute. The concentration gradient of semipermeable solute across the cell membrane forces the cell volume to expand, reaching a peak volume $V = V_{\mathrm{peak}}$ at time $t = t_{\mathrm{peak}}$ (see figure 9). This peak is achieved as a consequence of a balance between the drop in cellular salt concentration (as a result of the expansion of the cell) and the semipermeable solute concentration still relatively elevated within the cell. It is possible to deduce from this peak value alone both P_{sp} and L_{p} on the basis of the preceding analysis. This procedure involves *first* determining P_{sp} (independently of L_{p}), and *second* determining L_{p} as next described. (This procedure sharply contrasts with the existing methodology for determining membrane parameters (Gilmore 1996) using the so-called K–K model (Kedem & Katchalsky 1958).)

The ability to independently determine P_{sp} and L_{p} from the peak volume owes to the fact that two pieces of information are resident in the time (t_{peak}) of the peak volume: (1) the volume $V = V_{\mathrm{peak}}$; and (2) the time derivative of the radius $(\mathrm{d}R/\mathrm{d}t) = 0$. The equations for determining P_{sp} can be deduced from condition 1. Using (7.35)–(7.37), the following equation (implicit in P_{sp} and independent of L_{p}) holds:

$$\omega = 2\sum_{n=1}^{\infty} \frac{\sin^2(\lambda_n) - \lambda_n \sin(\lambda_n)\cos(\lambda_n)}{\lambda_n^2 - \lambda_n \sin(\lambda_n)\cos(\lambda_n)} \mathrm{e}^{-\lambda_n^2 x}, \tag{7.40}$$

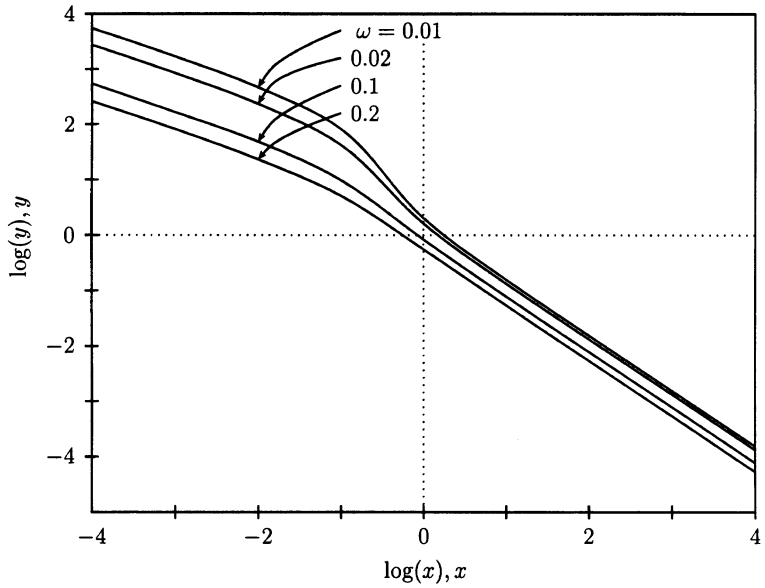

Figure 13. The semipermeable solute permeability P_{sp} (or y) can be uniquely determined from the peak quantities t_{peak} and V_{peak} appearing in the dimensionless variables x and ω.

with the eigenvalues being the non-zero roots of

$$\frac{\lambda_n}{1-y} = \tan(\lambda_n). \tag{7.41}$$

In the above, three dimensionless quantities have been defined:

$$x \stackrel{\mathrm{def}}{=} \overline{D}^*_{\mathrm{sp}}|_{\mathrm{peak}} \frac{t_{\mathrm{peak}}}{R^2_{\mathrm{peak}}}, \tag{7.42}$$

$$\omega \stackrel{\mathrm{def}}{=} \frac{C^{\mathrm{e}}_{\mathrm{salt}}[V_{\mathrm{peak}} - V_{\mathrm{b}}] - C^{\mathrm{i}}_{\mathrm{salt}}(0)[V_{\mathrm{i}} - V_{\mathrm{b}}]}{\sigma[C^{\mathrm{i}}_{\mathrm{sp}}(0) - C^{\mathrm{e}}_{\mathrm{sp}}]\,[V_{\mathrm{peak}} - V_{\mathrm{b}}]}, \tag{7.43}$$

$$y \stackrel{\mathrm{def}}{=} P_{\mathrm{sp}} \frac{R_{\mathrm{peak}}}{[1 + (3k/a + K - 1)\phi_{\mathrm{i}} V_{\mathrm{i}}/V_{\mathrm{peak}}]\overline{D}^*_{\mathrm{sp}}|_{\mathrm{peak}}}. \tag{7.44}$$

All the parameters appearing in these expressions (except for P_{sp} which is sought in the analysis) are known or measurable. The effective diffusivity $\overline{D}^*_{\mathrm{sp}}|_{\mathrm{peak}}$ can be obtained from (7.32) as

$$\overline{D}^*_{\mathrm{sp}}|_{\mathrm{peak}} = \frac{D^{\mathrm{cyt}}_{\mathrm{sp}}}{1 + (3k/a + K - 1)\phi_{\mathrm{i}} V_{\mathrm{i}}/V_{\mathrm{peak}}} \left[1 - \frac{3\phi_{\mathrm{i}} V_{\mathrm{i}}/V_{\mathrm{peak}}}{2 + 2\Gamma + (1 - 2\Gamma)\phi_{\mathrm{i}} V_{\mathrm{i}}/V_{\mathrm{peak}}}\right], \tag{7.45}$$

with the osmotically inactive volume fraction related to V by $\phi = \phi_{\mathrm{i}} V_{\mathrm{i}}/V$. By measurement of $\{t_{\mathrm{peak}}, V_{\mathrm{peak}}\}$, x and ω can be calculated directly from (7.42) and (7.43). This then allows for the solution of (7.40) and (7.41) for y, which in turn gives P_{sp} via (7.44). The relationship between x, ω and y is shown graphically in figure 13. The behaviour shown, and embodied in (7.40)–(7.44), is general for *any* homogeneous cell expansion/contraction, not simply that of the explicitly outlined protocol.

Having uniquely determined P_{sp} from the above, L_{p} can be calculated from the solution $\eta(\tau)$. This is an iterative procedure, involving selection of a value for L_{p},

Table 3. *Human sperm cell*
(Experimental data measured during the removal of cryoprotectant from human sperm.)

symbol	value	units
T	22	°C
V_i	28.2	μm^3
V_b	14.1	μm^3
D_{sp}^{cyt}	10^{-6}	$cm^2\ s^{-1}$
D_{sp}^{surf}	10^{-7}	$cm^2\ s^{-1}$
K	0	—
$C_{salt}^{i}(0)$	0.26	$mol\ l^{-1}$
C_{salt}^{e}	0.26	$mol\ l^{-1}$
C_{sp}^{e}	0	$mol\ l^{-1}$

	DMSO	ethylene glycol	glycerol	propylene glycol	
σ	0.98	0.77	0.93	0.95	—
$C_{sp}^{i}(0)$	1.0	2.0	1.0	1.0	$mol\ l^{-1}$
t_{peak}	2.50	1.58	1.21	1.20	s
V_{peak}/V_i	1.73	1.31	1.40	1.52	—

calculating the response $\eta(\tau)$, and determining values of t_{peak} and V_{peak}. The proper choice of L_p is obviously that which produces the measured values of t_{peak} and V_{peak}.

As a brief example, consider the base case, assume that P_{sp} and L_p are unknown. Assume that we measure a peak at time $t_{peak} = 20$ s of magnitude $V_{peak}/V_i = 1.5$. Solving (7.40)–(7.44) yields a value of $P_{sp} = 3.92 \times 10^{-3}$ cm min^{-1} (assuming $k/a = 1$) or a value of $P_{sp} = 1.67 \times 10^{-3}$ cm min^{-1} (assuming $k/a = 0$). The solution $\eta(\tau)$ can then be iterated to find that $L_p = 0.660$ and 0.698 μm min^{-1} atm^{-1} for $k/a = 1$ and 0, respectively.

(*f*) *Comparison with former model: human sperm*

An alternative approach to the theory outlined here is provided by the K–K model (Kedem & Katchalsky 1958). The K–K model differs from the present treatment in that it does not provide a detailed mass transport analysis of an expanding/contracting cell. It assumes the validity of equation (6.24) *a priori* (ideal osmometer assumption) and regards kinetic swelling as a volume response of cells to osmotic stimuli, *independent* of cell shape, or possible asymmetries in the system. It assumes instantaneous mixing of solute inside the cell, both for the cases of salt and semipermeable solute, thus neither solute diffusivity, cytosolic structure or absorption phenomena are accounted for in the K–K model.

In this section, the kinetic volume data collected by Gilmore *et al.* (1995) (and used, by them, to deduce values of P_{sp} and L_p on the basis of the K–K model for human sperm), are reinterpreted on the basis of the protocol described in the preceeding section. It is essential to note that human sperm are highly non-spherical (the osmotically active domain apparently being cylinder-like); nevertheless, application of the theory outlined here is not without some justification. First, the K–K model itself makes no distinction of the role of cell shape. Second, the method used by Gilmore *et al.* (1995) for measuring volume expansion is that of a Coulter counter which again is unable to discriminate between spherical and non-spherical cell shapes.

Table 4. *K–K model versus present model*

(A comparison of calculated values for P_{sp} and L_p using the least-squares type fit applied to the K–K model and the peak point calculation outlined here.)

			present model	
symbol	cryoprotectant	K–K model	$k/a = 0$	k/a=1
P_{sp} ($\times 10^{-3}$ cm min^{-1})	DMSO	0.8	2.39	5.31
	ethylene glycol	7.9	4.45	12.8
	glycerol	2.1	4.70	12.6
	propylene glycol	2.3	4.80	11.9
L_p (μm min^{-1} atm^{-1})	DMSO	0.84	1.28	1.17
	ethylene glycol	0.74	0.67	0.63
	glycerol	0.77	1.64	1.55
	propylene glycol	1.23	2.04	1.90

In contrast with the method for deducing P_{sp} and L_p from the K–K model (least-squares type fit adjusting both P_{sp} and L_p until the theoretical curve best approximates the experimental data), in the protocol outlined here only the experimentally determined t_{peak}, V_{peak} values are used. Having deduced P_{sp} and L_p on this basis, a *consistancy check* is then made by comparing the volume response for all t with the experimental data.

The relevant physical data for the human sperm cell and the various cryoprotectants are shown in table 3. Values for t_{peak} and V_{peak}/V_i (read from graphs) are also tabulated.

Table 4 shows the results for P_{sp} and L_p using both the K–K model and the protocol outlined in the previous subsection. The values of P_{sp} and L_p deduced here differ (both for $k/a = 0$ and 1) from those determined by the K–K model, though generally by less than an order of magnitude. Higher organelle absorption $k/a = 10$ or $k/a = 100$ leads to dramatic differences between the two theories. For example, the permeability, P_{sp}, of glycerol increases from $P_{sp} = 4.7\times10^{-3}$ at $k/a = 0$ to 86.2×10^{-3} at $k/a = 10$ and 953×10^{-3} at $k/a = 100$. These high absorption coefficients are, however, not expected at least for the cryoprotectants shown (see Diamond & Katz (1974) for representative lipid bilayer partition coefficients).

The results of table 4 reveal that unequivocal values of membrane permeation properties, in the presence of semipermeable solutes, require a detailed analysis, as outlined here, and that substantial errors can be made particularly if the semipermeable solute (as in the case of a cryoprotectant) is capable of absorbing significantly into the lipid bilayers of internal organelles.

Figures 14 and 15 show comparisons between the theoretical predictions of tables 3 and 4 and the experimental data in the cases of propylene glycol and DMSO. The reasonable agreement between theory and experiment lends support to the analysis as well as the protocol for determining P_{sp} and L_p from peak data.

8. Arbitrary cell shapes and future directions

The preceding analysis has dealt solely with the case of a spherical cell undergoing radial deformations. In general, anisotropic deformations of cell membranes, or at

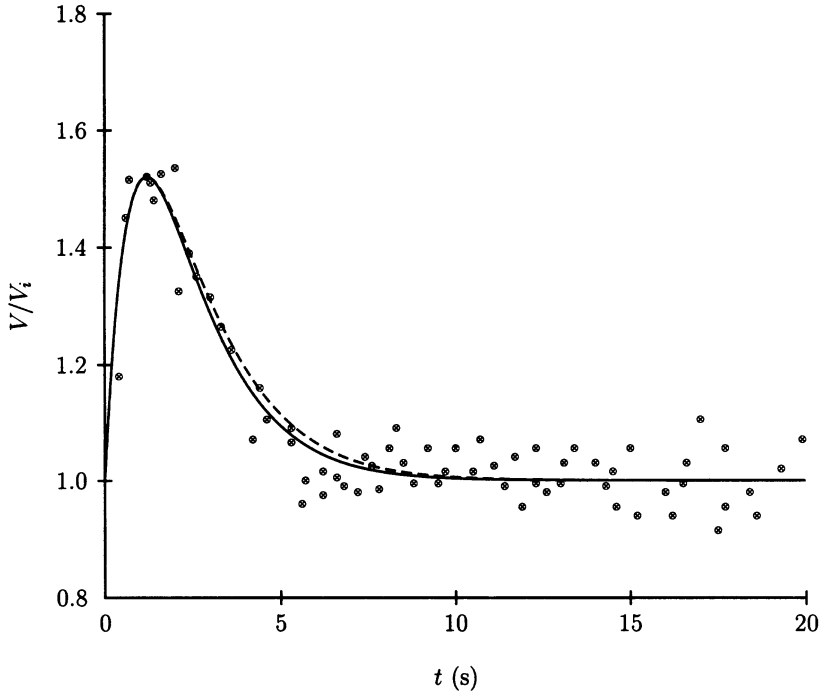

Figure 14. A comparison of experimental (human sperm) cell volume response with theoretical predictions for the case of propylene glycol. Experimental data taken from Gilmore *et al.* (1995).

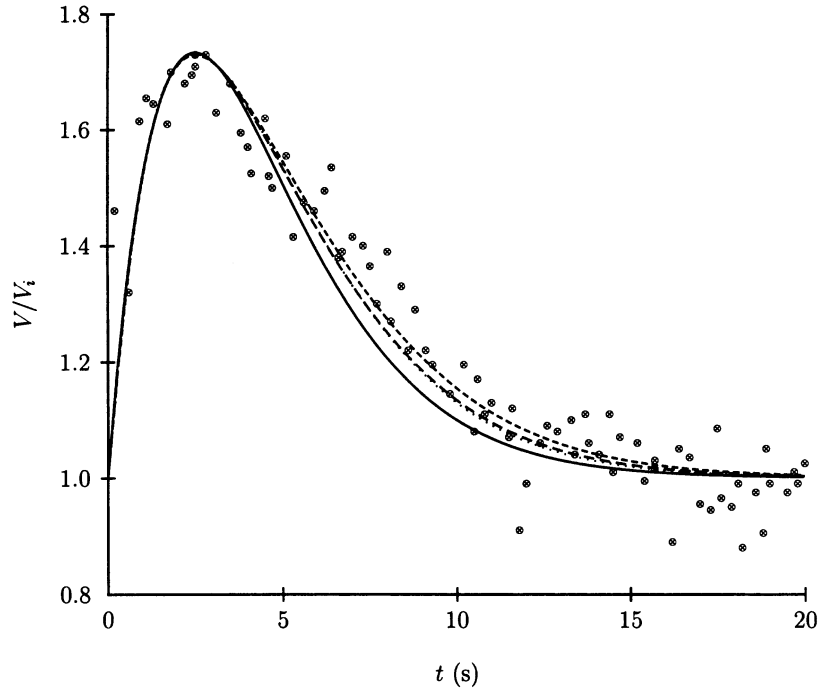

Figure 15. A comparison of experimental (human sperm) cell volume response with theoretical predictions for the case of DMSO. Experimental data taken from Gilmore *et al.* (1995).

least non-spherically isotropic deformations can be expected owing to non-spherical cell shapes and spatially inhomogeneous osmotic stresses. The comparisons made in § 7 *f* to sperm must be considered in this light preliminary until a more careful analysis of shape effects has been made.

In this final section, we discuss how the preceeding formalism may be generalized to address cases of non-spherical cell deformations, and consider possible future directions.

We begin with the case of a non-spherical cell suddenly exposed to anisosmotic conditions in the absence of a semipermeable solute. This is the case addressed in § 6 for a spherical cell undergoing a homogeneous osmotic stress. First note that for the case of an inhomogeneous deformation, or a non-spherical cell shape, the cellular fluid velocity $\boldsymbol{v}$ need *not* be zero (see § 2); however, $\boldsymbol{v}$ will scale with the velocity $\boldsymbol{u}$ of the cell membrane and, as such, the pseudo-steady-state approximations made earlier still hold. The generalization of (6.9)–(6.11) can then be written

$$\nabla^2 \overline{C}^{\mathrm{i}}_{\mathrm{salt}} = 0, \tag{8.1}$$

$$\boldsymbol{n} \cdot \nabla \overline{C}^{\mathrm{i}}_{\mathrm{salt}} = 0, \quad \forall (r \in \text{plasma membrane}), \tag{8.2}$$

where $\boldsymbol{n}$ is the instantaneous unit normal of the cell membrane. This problem has the trivial yet important solution

$$\overline{C}^{\mathrm{i}}_{\mathrm{salt}} = \frac{N_{\mathrm{salt}}}{V(t)} \tag{8.3}$$

or

$$C^{\mathrm{i}}_{\mathrm{salt}} = \frac{N_{\mathrm{salt}}}{V(t) - V_{\mathrm{b}}}, \tag{8.4}$$

which reduces to (6.12) and (6.13) in the limit of a sphere, $V = \frac{4}{3}\pi R^3$. The volume response of the cell is governed by (cf. (6.14) as well as (3.3)–(3.5))

$$\frac{1}{A(t)} \frac{\mathrm{d}V}{\mathrm{d}t} = -L_{\mathrm{p}} R_{\mathrm{gas}} T \left[C^{\mathrm{e}}_{\mathrm{salt}} - \frac{N_{\mathrm{salt}}}{V(t) - V_{\mathrm{b}}} \right], \tag{8.5}$$

subject to

$$V = V_{\mathrm{i}}, \quad \text{at } (t = 0) \tag{8.6}$$

and with a known relationship between $V(t)$ and $A(t)$. Equations (8.5) and (8.6) can be solved for $V(t)$, knowing $C^{\mathrm{e}}_{\mathrm{salt}}$, as has been done elsewhere (Gilmore *et al.* 1995).

In the case wherein a semipermeable solute is also present, equations (7.12)–(7.15) assume the forms

$$\frac{\partial C^{\mathrm{i}}_{\mathrm{sp}}}{\partial t} = \overline{D}^{*}_{\mathrm{sp}} \nabla^2 C^{\mathrm{i}}_{\mathrm{sp}}, \tag{8.7}$$

$$\overline{D}^{*}_{\mathrm{sp}} (1 - \phi + k\alpha + K\phi) \boldsymbol{n} \cdot \nabla C^{\mathrm{i}}_{\mathrm{sp}} = P_{\mathrm{sp}} (C^{\mathrm{e}}_{\mathrm{sp}} - C^{\mathrm{i}}_{\mathrm{sp}}), \tag{8.8}$$

$$C^{\mathrm{i}}_{\mathrm{sp}} = C^{\mathrm{i}}_{\mathrm{sp}}(0), \quad \text{at } (t = 0). \tag{8.9}$$

This boundary-initial-value problem possesses a non-trivial solution that is strongly dependent on instantaneous cell shape. The result for the important case of a cylindrical membrane is discussed in a subsequent article (Batycky *et al.* 1998).

In addition to generalizing the foregoing to non-spherical membrane deformations, fruitful avenues of future theoretical inquiry might include the roles played by closely neighbouring cells in multicell assemblages on osmotic expansion and contraction,

'slow' or 'perturbation' expansions or contractions of cells that can be influenced by active membrane transport mechanisms, simultaneous heat transfer (and ice formation) in non-isothermal environments, and shifts in metabolic reaction equilibria. It is nonetheless key that theoretical analyses be accompanied by reasoned experiments whereby theoretical postulates can be tested and new unexpected phenomena revealed. In this context, particularly in light of the present study, an experimental study aimed at quantifying the degree of intracellular membrane absorption for a variety of cryoprotectants is clearly necessary.

This work was partly supported by NIH grant HD 093-13. D.A.E. acknowledges support provided by an NSF CAREER Grant Award.

References

Abramowitz, M. & Stegun, I. A. 1972 *Handbook of mathematical functions.* New York: Dover.

Alberts, B., Bray, D., Lewis, J., Raff, M., Roberts, K. & Watson, J. D. 1994 *Molecular biology of the cell*, 3rd edn. New York: Garland.

Aris, R. 1962 *Vectors, tensors and the basic equations of fluid mechanics.* Engelwood Cliffs, NJ: Prentice-Hall.

Bashford, C. L., Adler, G. M., Menestrina, G., Micklem, K. J., Murphy, J. J. & Pasternak, C. A. 1986 Membrane damage by hemolytic viruses, toxins, complement and other cytolytic agents. *J. Biol. Chem.* **261**, 9300–9308.

Batycky, R. P., Kang, S., Hammerstedt, R. & Edwards, D. A. 1998 Interpretation of osmotic challenge experiments: towards a protocol. (In preparation.)

Brenner, H. & Edwards, D. A. 1993 *Macrotransport processes.* Boston, MA: Butterworth-Heinemann.

Camacho, J. & Brenner, H. 1995 On convection induced by molecular diffusion. *I&EC Res.* **34**, 3326–3335.

Carruthers, A. & Melchior, D. L. 1988 How bilayer lipids affect membrane activity. *TIBS* **11**, 331–335.

Clegg, R. M. & Vaz, W. L. C. 1985 Translational diffusion of proteins and lipids in artificial lipid bilayer membranes. A comparison of experiment and theory. In *Progress in lipid–protein interactions* (ed. A. Watts & J. J. H. dePont), pp. 173–229. New York: Elsevier.

Courtens, J. L. & Paquignon, M. 1985 Ultrastructure of fresh, frozen and frozen-thawed spermatozoa of the boar. *1st Int. Conf. on Deep Freezing of Boar Semen. Uppsala, Sweden*, pp. 61–87. Swedish University of Agricultural Sciences.

Darcy, H. P. G. 1856 *Les fontaines publiques de la ville de Dijon.* Paris: Victor Dalmont.

Diamond, J. M. & Katz, Y. 1974 Interpretation of nonelectrolyte partition coefficients between dimyristoyl lecithin and water. *J. Membrane Biol.* **17**, 121–139.

Edwards, D. A. & Davis, A. M. J. 1995 Diffusion and convective dispersion through arrays of spheres with surface adsorption, diffusion and unequal solute partitioning. *Chem. Engng Sci.* **50**, 1441–1454.

Foote, R. H. 1984 Buffers and extenders, What do they do? Why are they important? *Proc. X NAAB Tech. Conf. AI Reprod.*, 62–70.

Frankel, I., Mancini, F. & Brenner, H. 1991 Sedimentation, diffusion, and Taylor dispersion of a flexible fluctuating macromolecule: the Debye–Bueche model revisited. *J. Chem. Phys.* **95**, 8636–8646.

Gao, D. Y., Mazur, P., Kleinhans, F. W., Watson, P. F., Noiles, E. E. & Critser, J. K. 1992 Glycerol permeability of human spermatozoa and its activation energy. *Cryobiol.* **29**, 657–667.

Gilmore, J. A., McGann, L. E., Liu, J., Gao, D. Y., Peter, A. T., Kleinhans, F. W. & Critser, J. K. 1995 The effect of cryoprotectant solutes on water permeability of human spermatozoa. *Biol. Reprod.* **53**, 985–995.

Hammerstedt, R. H., Graham, J. K. & Nolan, J. P. 1990 Cryopreservation of mammalian sperm: what we ask them to survive. *J. Androl.* **11**, 73–88.

Kedem, O. & Kalchesky, A. 1958 Thermodynamic analysis of the permeability of biological membranes to nonelectrolytes. *Biochem. Biophys. Acta.* **27**, 229–246

Liu, C., Gao, D. Y., McGann, L. E., Benson, C. T., Critser, E. S. & Critser, J. K. 1995 The high water permeability of human spermatozoa is mercury resistant and not mediated by CHIP28. *Biol. Reprod.* **52**, 913–919.

Mazur, P. 1984 Freezing of living cells: mechanisms and implications. *Am. J. Physiol.* **247**, C125–142.

Mazur, P., Rall, W. F. & Liebo, S. P. 1984 Kinetics of water loss and the likelihood of intracellular freezing in the mouse ova. *Cell Biophys.* **6**, 197–213.

O'Leary, T. J. & Levin, I. W. 1984 Ramen spectroscopic study of an interdigitated lipid bilayer dipalmitoylphosphatidylcholine disperse in glycerol. *Biochem. Biophys. Acta* **776**, 185–189.

Patton, J. 1996 Mechanisms of macromolecule absorption by the lung. *Adv. Drug Deliv. Rev.* **19**, 3–36.

Press, W. H., Teukolsky, S. A., Vetterling, W. T. & Flannery, B. P. 1994 *Numerical recipies in FORTRAN*, 2nd edn. Cambridge University Press.

Quinn, P. J. 1989 A lipid-phase separation model of low-temperature damage to biological membranes. *Cryobiol.* **22**, 128–142.

Watson, P. F. 1990 Artificial insemination and the preservation of semen. In *Marshall's physiology of reproduction* (ed. G. E. Lamming), 4th edn, vol. 2, pp. 748–869. London: Churchill Livingston.

Received 17 May 1996; accepted 24 February 1997